Grid Stability Studies of Electrolyzer-based Energy Storage Integration

Adam Pramana Fitrah

Faculty of Engineering and Science
Electrical Power Systems and High Voltage Engineering

Master Thesis, EPSH4-1034, 2022-05

STUDENT REPORT
AALBORG UNIVERSITY

Grid Stability Studies of Electrolyzer-based Energy Storage Integration

Adam Pramana Fitrah

Faculty of Engineering and Science
Electrical Power Systems and High Voltage Engineering

Master Thesis, EPSH4-1034, 2022-05

Software used in the project: DIgSILENT PowerFactory. The thesis project is in collaboration between Aalborg University and Energinet

AALBORG UNIVERSITY
STUDENT REPORT

AAU Energy
Aalborg University
http://www.aau.dk

Title:
Grid Stability Studies of Electrolyzer-based Energy Storage Integration

Theme:
Scientific Theme

Project Period:
Spring Semester 2022

Project Group:
EPSH4-1034

Participant(s):
Adam Pramana Fitrah

Supervisor(s):
Claus Leth Bak
Filipe Miguel Faria Da Silva

Page Numbers: 71

Date of Completion:
May 30, 2022

Abstract:

Denmark has set to a full renewable energy system for electricity and heating in the coming years where RE share in Denmark has reached 68% in 2020. However, there are challenges to realize the green transition as the renewable energy sources may prompt to disturbances in the system compared to conventional energy plant. One of the ideas is by deploying energy storage that converts electricity into other form of energy. This is known as power-to-x (PtX) technology. However, the deployment of PtX in the grid system may affect the stability in case disturbances occur in the system. Thus, this project is intended to model the PtX technology and its dynamic behaviour to investigate the impact of the PtX integration in the grid system. Several schemes to study the response of the system due to the integration of PtX is simulated, such as symmetrical fault and asymmetrical fault injection and loss of generation unit. The results obtained show that the developed PtX model could provide services to the system and improve the frequency and voltage performance.

Preface

This master's thesis is written by a 4th-semester MSc student with specialisation Electrical Power Systems and High Voltage Engineering at the Department of Energy Technology, Aalborg University, Denmark. The thesis discusses the impact of Power-to-X technology in the grid system where the controller of the Power-to-X plays an important role in controlling the output of the developed model. The thesis project was proposed by Danish transmission system operator, Energinet.

The author would like to thank Claus Leth Bak and Filipe Faria da Silva, as the supervisors, and Jacob Bollerslev, as the co-supervisor from Energinet, for the discussions and ideas throughout the project.

Readers' Guide

This thesis report is written systematically, meaning that the chapters and sections are in order for the readers to understand the topic clearly. Citations used in this report is based on the IEEE format where the bibliography is placed after the last chapter of the report. The figures, tables, and equations are named chronologically based on its appearance in the report. DIgSILENT PowerFactory software is used to model and simulate the test cases in this project.

Contents

List of Figures

List of Tables

Chapter 1

Introduction

1.1 Background

The energy transition to carbon-neutral system has attracted the world's attention in the past few years and will continue in the coming years. The European Union (EU) aims to reduce 80% of its domestic emissions in 2050 compared to 1990 [1]. In line with the EU goal, Denmark through its government and parliament set an ambition to lower the carbon emission by 70% below the 1990 level at 2030 as a step to reach carbon-free in 2050 [2]. To support this action, the Danish government is targeting a 100% renewable energy (RE) system for electricity and heating [3], where already RE share in Denmark's electricity supply has reached 68% in 2020 [4].

The transition to green energy sources will result in a better environment for mankind to live; however, this also requires technical support as it faces challenges, mainly due to the varying power of RE sources, such as wind and solar, making it hard to predict the output power [5]. This phenomenon happens because RE varies depending on the weather and season leading to the mismatch between the demand and supply of energy. Thus, it would be beneficial to deploy different type of energy storage, taking into consideration the advantageous and disadvantageous of each type, to enable higher penetration of RE on the system. This action helps in realizing green and sustainable energy systems.

Pumped hydro energy storage (PHES), compressed air energy storage (CAES), batteries, flywheel, Power-to-X (PtX) are the example of energy storage applications. Focusing on the PtX, the technology could satisfy energy demand, not only for electricity, but also for heating, transport, and industry. As a promising technology to store energy for long term solutions, PtX has several characteristics such as high storage capacity, high volumetric storage density, ability to provide grid services, and storage duration compared to the traditional energy storage, like PHES [6].

Denmark, in particular, has been focusing on PtX technologies as part of its future energy system implied by the strategies for PtX and hydrogen and also the number of PtX projects, where PtX is seen crucial to further de-carbonize the energy system [7–10]. The report from Danish Government stated that Denmark could potentially become a global player in PtX technology as many Danish industries working on the research and development of PtX and carbon capture, utilisation, and storage (CCUS) technology involving universities and institutions. This collaboration could lead to inventions and innovations at the study of the respective technology and make the technology mature rapidly. Also, the abundant amount of wind resources in Denmark benefits the condition of PtX implementation, that could be used for producing green hydrogen and other gasses, which requires large amount of electrical energy [11].

One of the on-going projects utilizing PtX technology in Denmark is the energy island projects located in the North sea and Baltic sea with total capacity of 5GW initially. Denmark plans to create these artificial energy islands exploiting the wind energy resources to power the grid and also transform the electricity produced from renewable energy to other energy carriers with the help of PtX technology [12].

Power-to-X as energy storage

PtX is a technology converting molecules, such as water, into other energy carriers with the help of electrolysis process. The products of this chemical reactions from electrolysis acts as energy storage where it can be deployed to meet the energy demand of electricity, transport, heating and helps in further decarbonization of energy systems [13]. The "X" term stands for the product obtained from electrolysis, like hydrogen and ammonia. Figure 1.1 illustrate the schemes of PtX technologies in several applications. To help the transition of energy into green energy, the electricity used in the process may be generated from renewable power plants, such as wind and solar. The feedstock used in the electrolysis process can be water or carbon dioxide or nitrogen dioxide captured from the environment.

PtX technology offers many possibilities as it can produce hydrogen, synthesis gas, ammonia, and hydrogen peroxide depending on the feed stock. Furthermore, the produced chemical molecules in the primary stage could be used for other reactions to obtain another form of energy carriers. The produced hydrogen could be used for process of methanation, hydrogenation, Fischer-Tropsch for hydrocarbon production, and Haber-Bosch for generating ammonia. The same also goes for the produced synthesis gas where it is used for chemical reaction for producing methane and Fischer-Tropsch process.

The main component of PtX system is the electrolysis which can be used for water electrolysis, methanol electrolysis, and other applications of electrolysis. Several types of electrolyzer have been developed, such as alkaline electrolyzer, proton

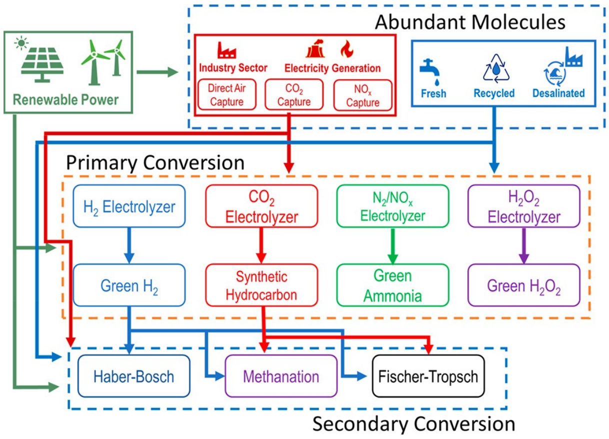

Figure 1.1: Power-to-X possible schemes [13]

exchange membrane electrolyzer, and solid oxide electrolyzer [13, 14]. The perfomance of these technologies also differ depending on the feedstock, e.g water and methanol [15]. The detail explanation of these technologies are presented in chapter 2.

The PtX system requires an AC-DC converter to be integrated to the grid as PtX operates at DC power [16]. Thus, the whole PtX system can be considered as converter-based technology where it is used to store electricity into other energy carriers and for particular electrolyzer technology, it can also be used to power the grid back. Integration of such technology to the power systems is challenging as from the system perspective, the concern is related to the inertia, voltage and frequency fluctuations, fault current contribution, to ensure the grid stability and security of supply [17, 18]. Thus, controllers are necessary for the energy storage to be connected so that it could operate at the allowable operation range as regulated by the system operator. Also, the controls of energy storage would help the equipment to remain connected to the system without losing synchronisation if disturbances occur in the system. Studies also mentioned that PtX or hydrogen storage could provide ancillary service, such as voltage support and frequency response, and enhance the flexibility of the grids [19–22]. Figure 1.2 shows the regulation from Energinet for balancing power where the energy storage should be able to have such functionality to activate and deactivate an increase or decrease of power from and to the energy storage system [20].

In electrical modelling, the electrolyzer could be modelled as load connected to the converter interfacing the electrolyzer to the grid where the controllers, such as power and current control, are included as in [23–26]. The electrolyzer model representation would be explained more in detail in Chapter 2.

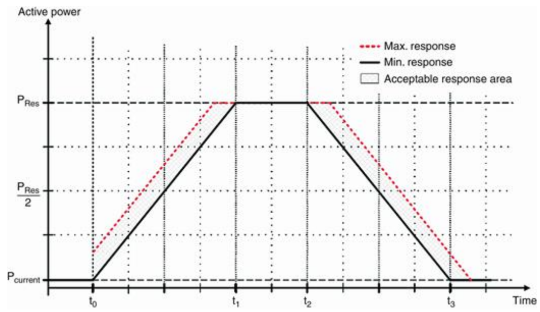

Figure 1.2: Frequency containment reserve regulation from Energinet [20]

Grid code requirement

To deploy the PtX facilities to the electrical grid, the developer needs to fulfil the grid code requirement regulated by the transmission system operator (TSO), i.e. Energinet. PtX technology is considered as energy storage facility and thus, it would have different requirements to be fulfilled compared to other types of power-generating plants [27].

There are several requirements needed to satisfy for the energy storage to be able to get connection to the grid where more detail information can be accessed in [27]. The requirements needed to be fulfilled by the energy storage's owner depend on the energy storage's site area, whether it is located at western or eastern Denmark. This is because Danish's electrical grid system consists of two grids: DK1 (western) and DK2 (eastern). The requirements for both grid, in principal, are the same where the difference is on the value range criteria. Below is the requirement from Energinet for voltage deviation for energy storage facilities.

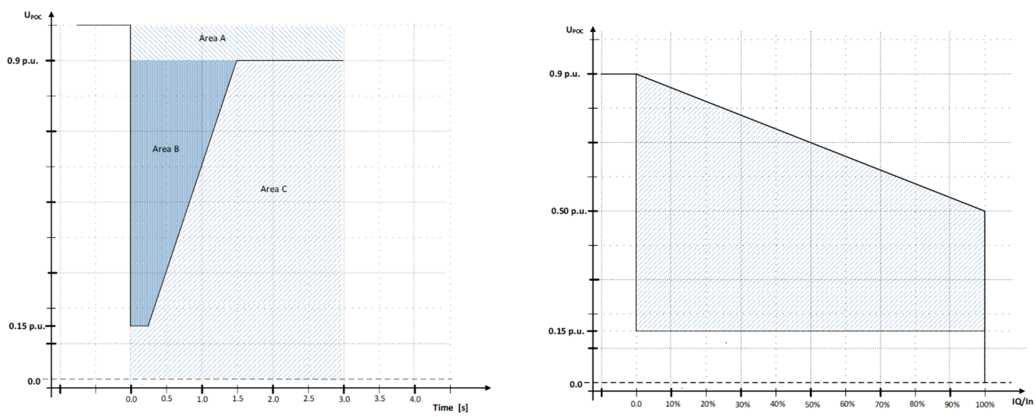

Figure 1.3: Requirements of tolerance to voltage dips (left) and supply of fast fault current (right) [27]

Figure 1.3 shows the requirement needed for energy storage when the voltage dips occurs. The energy storage should maintain its normal operation inside area A, while it also should be still connected to the grid system by providing voltage support. Voltage support is realized by supplying reactive current to the grid and the minimum criteria for supplying reactive current is shown on the right figure of Figure 1.3. If the voltage at the POC falls to area C, it is allowable for the energy storage to disconnect from the grid.

Another requirement from the TSO is the frequency response regulation where the energy storage should be able to increase its output power if the frequency drops below its minimum frequency setting (under-frequency condition) and also decrease its output if the frequency increases higher than its maximum setting (over-frequency). Moreover, there is a requirement for energy storage to have frequency control (FSM) function implemented. Reactive power control and power factor control should also be implemented with an addition of automatic power factor control or voltage control functionality depending on the classification of energy storage.

The simulations required to be done in general are static, root-mean-square (RMS), and harmonic simulation while for larger capacity of energy storage should also provide transient simulation. Fault injection or the change of frequency in the system could be taken to show the response of the energy storage towards such conditions. The energy storage facility should be able to perform these studies and comply with the requirements [27].

This study project only discusses the simulation for dynamic (RMS) simulation and investigate the response of such storage due to the integration to the power grid system.

1.2 Problem statement

As the electrical grid is experiencing a transition towards a dominant RE system from the dominant conventional power plants, the technologies employed should be able to have grid support services to support the grid in order to still operate at the allowed operation ranges. These operation regulations are regulated by the transmission system operator. One of the promising green technologies is PtX technology which can store energy by transforming electrical energy into other energy carriers and later be used in many applications, such as transport, heating, and electrification. In order to integrate the PtX system to the power systems, the PtX needs to fulfill the grid code requirements determined by the system operator. Hence, it is necessary to develop a general plant model that is able to show the behavior of the PtX plant. In this project, the model developed is intended to be able to show the dynamic (RMS) response, such as the voltage deviations, by performing grid stability studies.

1.3 Project objectives and methodology

The aim of the thesis project can be described as to build a PtX dynamic simulation model and later perform grid stability study to investigate the impact of the integration of the developed model on grid system, focusing on the voltage stability.

To achieve the objectives of the project, the following actions need to be taken:

1. Investigate and describe the state-of-the-art for PtX technology with respect to the grid integration with a focus on a dynamic model for studying the impact on the power system stability
2. Design a generic dynamic PtX model based on the functional and model requirements
3. Implement the model in PowerFactory
4. Perform stability studies to see the response of the system towards the integration of PtX for different selected study cases
5. Discuss and evaluate the generic dynamic PtX model and draw general guidelines on PtX impact on system stability

The software used for the electrical simulation studies is DIgSILENT Powerfactory.

1.4 Scope and limitations

There are some limitations taken into consideration in working on this project. As the project only aims to see the dynamic response (RMS) on the system due to the integration of PtX plant, the physical chemical reactions of the plant is not a matter in this project. The limitation of the project includes:

- Electrolyzer of the PtX system is modelled as generic load with its corresponding dynamic model
- The loads modelled in the PtX system are passive loads
- Converter parameters are taken from existing data/template
- The grid system used for test study is generic grid

1.5 Outline of project report

The outline of this report is structured as follows:

Chapter 1: This chapter gives the introduction of the project, motivation, and its scope and constraints.

Chapter 2: This chapter describes the state of the art of PtX technology and the power electronics used to interface the electrolyzer to the grid syste. Besides, background theory of the stability the simulation techniques are discussed.

Chapter 3: In this chapter, the explanation on the modelling of the system test in this project, IEEE 9-bus system, is explained. This includes the modelling of the dynamic behaviour of the generators.

Chapter 4: The main discussion of this chapter is the modelling of the PtX model which includes the modelling of the controller of the PtX.

Chapter 5: This chapter discuss the impact of the PtX integration on the IEEE 9-bus system. Several simulation schemes are presented in this chapter to show the response of the system towards the integration of the PtX.

Chapter 6: This chapter summarizes and concludes the result obtained and also the future work or study could be done based on this project.

Chapter 2

State-of-the-Art

In this chapter, the development of PtX technologies is discussed where the control strategy used for the converter connecting the electrolyzer stack to the grid system is also presented. The control of the electrolyzer converter includes the power and current control to give reference to the converter. The stability issue in the power system is covered in this chapter with a focus on voltage stability. Lastly, the simulation techniques, like RMS and transient simulation, that can be used to help showing the response of such technologies in large scale system is covered.

2.1 Power-to-X system

As energy system transitioning to green energy, energy storage plays an important role enabling higher renewable energy sources integration to the electrical grid system. One of potential technologies to store energy for a long time is PtX technology where the energy stored can be used for many applications, like heating, transport, and re-electrification [28].

PtX system is consisted of two main parts: electrolyzer and power converter. Electrolyzer splits water into hydrogen and oxygen by electrolysis process. The electrolyzer operates by taking DC power and thus it is necessary to have converter interfacing the electrolyzer to the electrical grid system.

2.1.1 Electrolyzer

In principal, electrolyzer technology is similar to fuel cell but it works in its reverse process. Fuel cell needs hydrogen and oxygen as the feedstock to generate power while electrolyzer utilizes water as the source and with electricity, it produces hydrogen and oxygen. The feedstock of the electrolyzer does not have to be water, it can also be hydrocarbon; however, the utilization of water electrolyzer could also help in avoiding the emission of carbon dioxide as the end product of the electrolysis process [29].

There are various types of electrolyzer have been developed worldwide. Three most-known electrolyzer tecnologies are alkaline electrolyzer, proton-exchange membrane (PEM) electrolyzer, and solid oxide electrolyzer cell (SOEC) [30]. In the following subsections, a brief explanation of the electrolyzer technologies is presented.

Alkaline electrolyzer

Alkaline electrolyzer has been used for decades for large-scale industrial applications and it is the most mature technology for hydrogen generation, operating at low temperature and atmospheric pressure. The anode and cathode are separated by diaphragm conducting hydroxide ions OH^- with potassium hydroxide KOH solution [31, 32]. The chemical process of the alkaline electrolyzer is described in Figure 2.1 (a). In the cathode, the water is decomposed to hydroxide ions and hydrogen while the hydroxide ions gain energy from the electron and compose to oxygen and water at the anode.

Although its possibility to build large-scale hydrogen facility with this type of electrolyzer, it has a downside where the diaphragm causes losses and thus limits the current density. It also cannot fully separate the hydrogen and oxygen. However, alkaline technology offer an affordable cost to construct the electrolyzer [31].

PEM electrolyzer

The development of PEM electrolyzer is still new compared to alkaline electrolyzer, where PEM electrolyzer has an anode and cathode separated by a polymer electrolyte membrane. Similar to alkaline electrolyzer, PEM electrolyzer also operates at low temperature. The difference of PEM technology with other electrolyzers on the electrolysis process is the water fed to the anode instead of the cathode. PEM electrolyzer was developed to overcome the disadvantage of alkaline electrolyzer as PEM electrolyzer has high power density and cell efficiency and flexibility operation. Nevertheless, the initial cost to utilize PEM technology becomes the obstacle as it is quite expensive [32].

Mostly, PEM electrolyzer is applicable for small applications; however, in recent years, Siemens have developed hydrogen generation facility with PEM technology operating at MW-scale power, called Silyzer 300 [33]. The chemical reactions of PEM electrolyzer is shown in Figure 2.1 (b). The anode decomposes the water into hydrogen ions H^+ and due to the conducting characteristic of the electrolyte used in the process, it enables the ions to travel to cathode side and forms hydrogen.

SOEC electrolyzer

Solid oxide electrolysis (SOEC) electrolyzer is the latest developed electrolyzer compared to alkaline and PEM electrolyzer as SOEC is still in the research stage. The difference between SOEC and other electrolyzers is it operates at high temperature [29]. The electrolyte used as the medium in the electrolysis process might be oxygen-ion conducting electrolyte and proton-conducting electrolyte where these electrolytes are expected to have a high conductivity and enable the electrolyzer to operate at high temperature [34]. The reaction process of SOEC electrolyzer is shown in the Figure 2.1 (c).

The cathode of SOEC is feed with gas water where it gets ionized and split into hydrogen and oxide ions. While the hydrogen is formed in the cathode, the oxide ions goes to the anode and forms oxygen molecules. The advantages of this type of electrolyzer is it has high electrical efficiency, lower material cost and the flexibility to operate reversely as a fuel cell, where other electrolyzers do not have this functionality [32]. However, as its high-temperature operation, it may have some challenges, such as longer start-up/break-in times, mechanically unstable due to thermal stress, and also degradation of the equipment [34].

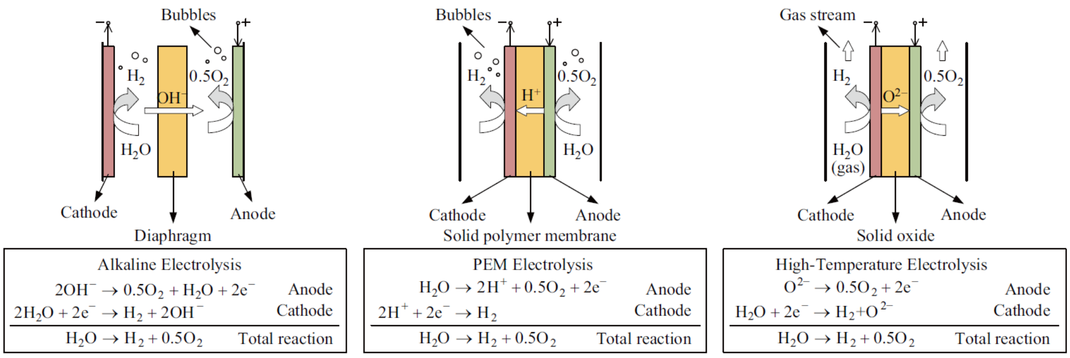

Figure 2.1: Chemical reactions of (a) Alkaline (b) PEM (c) SOEC electrolyzers [30]

Overview of electrolyzer technologies

According to [32], experts believe that the use of PEM electrolyzer will increase and shift out the alkaline electrolyzer due to the reduction of cost coupled to its operations flexibility and higher efficiency. Whereas, SOEC can be also the promising technology utilized in the coming years as it offers possibility to operate as both electrolyzer and fuel cell where the other two technologies cannot provide this functionality.

Dynamic characteristics of electrolyzer for providing grid services are load flexibility and the response time under sudden change conditions.The electrolyzer should also be able to provide grid services with certain response time. Normally, the response time of the electrolyzer is determined by the power electronic's capability interfacing the electrolyzer to the electrical grid as it is not limited by the stack capability [35]. This means the power electronic used for the electrolyzer should be adequate characteristic of the electrolyzer.

The report of [35] also stated that PEM technology would have quicker response time compared alkaline electrolyzer. Table 2.1 summarizes the characteristics of the three electrolyzer technologies based on report from [30, 32]. It shows that recent developments of electrolyzer technologies (PEM and SOEC) are able to have faster response and also having higher efficiency compared to alkaline electrolyzer.

Table 2.1: Characteristics of Alkaline, PEM, and SOEC electrolyzer

Characteristic	Alkaline	PEM	SOEC
Charge carrier	OH^-	H^+	O^{2-}
Current density [A cm^{-2}]	0.2 - 0.4	0.6 - 2.0	0.3 - 2.0
Cell voltage [V]	1.8 - 2.4	1.8 - 2.2	0.7 - 1.5
Operating temperature [°C]	60 - 80	50 - 80	650 - 1000
Operating pressure [bar]	<30	<200	<25
System efficiency [%]	55 - 67	60 - 70	90 - 95
Minimum load [%]	30 - 40	0 - 10	0 - 10
Dynamic response	Slow	Fast	Fast
Phase	Mature	Commercial	Demonstration

The equivalent electrical circuit of electrolyzer can be modelled as in Figure 2.2. This model can represent electrolyzer in general as each technologies mentioned are similar for their electrochemical model. There is a bit difference for SOEC electrolyzer as it operates at high temperature enabling it to have lower voltage and thus have a better efficiency [30].

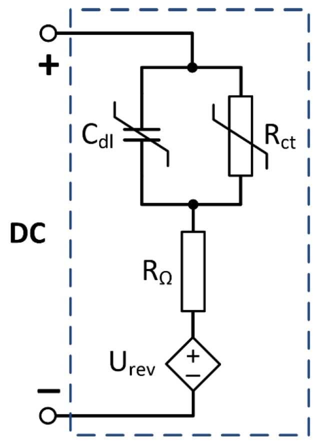

Figure 2.2: Equivalent electrolyzer model [16]

U_{ref} and R_{Ω} represent the reverse voltage and membrane resistance where these variables are temperature and pressure dependent to electrolyzer stack [16, 25]. The minimum energy required due to the reaction on the electrolyte defines the reverse voltage U_{ref}. On the other hand, the irreversible voltage is the required extra energy to make the electrolysis process occur, represented by other branches in Figure 2.2 [30].

The charge transfer resistance and double layer capacitor, which are dependent to temperature, are denoted with C_{dl} and R_{ct}. These components cause delay in the response of the electrolyzer as they behave like a limiter to electron flowing in the stack. However, it can be assumed that the delay in the control system or the chemical process of the units is negligible [36]. This is due to the small time constant leading to fast response of electrolyzer.

2.1.2 Power electronics

Power converter is used to interface the electrolyzer stack with the electrical grid system where the implemented power converter could be single stage (AC-DC conversion) or two stages (AC-DC-DC conversion). The power converter should include the control function of active and reactive power enabling the electrolyzer to operate at its capability. The control of electrolyzer converter can be described with the power control and current control where the current reference is generated from active and reactive power reference. Droop function also could be included to enable reducing the power [24].

The active power of the electrolyzer could be controlled with droop characteristics. As the electrolyzer is considered as a load, an inverse droop characteristic is used instead of the conventional droop characteristic for generation. Figure **??** shows the active power-frequency relation based on the droop function for electrolyzer applications. If the frequency increases, the electrolyzers will absorbs more active power and if the frequency decreases, the electrolyzer reduces its power consumption.

In [25], the active power of the electrolyzer is controlled based on the active power-frequency characteristics.

Several configurations of converter for electrolyzer applications have been developed. Report [16] studied the performance of 12-pulse thyristor rectifier (12-TR), 12-pulse diode rectifier with multi-phase chopper (12-DRMC), 12-pulse thyristor rectifier with active shunt power filter (12-TRASPF), and active front-end (AFE) rectifier for electrolyzer applications. The result shows that 12-TR has better performance for efficiency, reliability, and less complex, and lower cost compared to other topologies. However, 12-TR has an issue with the power quality, especially for condition of large-firing angle. 12-DRMC has better performance on the power quality compared to 12-TR but it still needs harmonic filter to lower the input harmonics. The 12-TRASPF is a hybrid concept of the previous mentioned topologies so it has better power quality, but the cost of this technology is higher with lower efficiency. The AFE rectifier address the power quality issue as it has the best performance on this matter. However, the control mechanism for AFE is more complex with higher cost too [16].

The converter model for electrolyzer could be modelled as grid forming converter or grid following converter [37]. The control strategy implemented for these converters would be different as the grid forming converter has purpose to "form" the grid by regulating the voltage and grid following converter regulates the output power. In this project, the model considered is grid following converter where the regulation of this type of converter could be help with the implementation of reverse droop characteristic, shown in Figure 2.3.

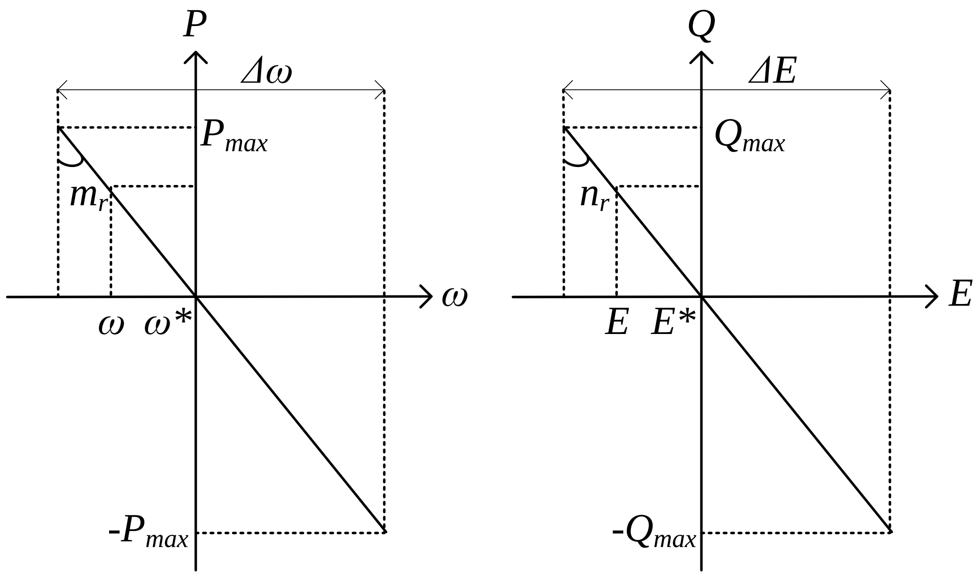

Figure 2.3: Power characteristic based on reverse droop control

2.2 Power system stability

The increasing growth of renewable energy technologies in the grid system brings challenges such as the stability issue. Power system stability is seen to be crucial matter in order to secure the operation of the electrical grid systems. By definition, power system stability means the ability of a system to remain operating at the equilibrium under normal condition and recover to the acceptable state after a disturbance. The stability of power system can be classified into rotor angle stability, frequency stability, and voltage stability [38].

Voltage stability

Voltage stability defines the ability to maintain steady voltage at all buses in the system after disturbance from a given initial operating condition while rotor angle stability is the ability of synchronous machine of an interconnected power system to remain in synchronism condition [38]. It can be said that voltage stability is load stability while rotor angle stability is generator stability. There is a term known as voltage collapse, a process following the voltage instability leading to blackout or abnormal low voltage in the system. If the voltage collapses at the transmission distant from the load area, it can assumed as the angle instability whereas if the voltage collapses in load area, it is determined as the voltage instability issue [38, 39].

Voltage stability can be classified into large disturbance and small disturbance voltage stability. Large disturbance voltage stability is the ability to maintain steady voltage due to large disturbance like system fault, loss of generation, or circuit contingencies. Small disturbance voltage stability indicates the ability to maintain steady voltages after small disturbances, like an increase of system load. Based on the time frame for voltage stability, it is divided into: short-term and long-term voltage stability. The time interest of short-term is in the order of several seconds involving fast acting load components, like controlled loads, induction motors, and converters. Whereas, the long-term is in the order of minutes involving slower acting components, like tap-changing transformer and generator current limiters [38].

The issue of voltage stability with dominant power electronic-interface technology in the grid system is mainly due to the limitation of reactive power and low short-circuit capacity following the curtailment of synchronous machines. The grid system should have sufficient reactive power to deliver to the load to maintain its stable condition, otherwise the system runs unstable. Equation 2.1 shows the relation of the reactive power supply to the demand [40].

$$Q_s(v) = \sqrt{[\frac{EV}{X_L}]^2 - [P_L(v)]^2} - \frac{V^2}{X_L} \tag{2.1}$$

$Q_s(v)$ is the reactive power supplied to the load through a line with reactance of X_L where E is the voltage source and V_L is the load voltage and active power demand of the load denoted as P_L.

2.3 Simulation modelling technique

With the increasing number of converter-based technology integrated into the power system, the network becomes more complex than ever. To secure a reliable operation of the system under such conditions, advanced power system modelling and techniques are required. For instance, the developed simulation model can be used to show the dynamic response accurately. In general, power system transient can be classified into three time-frame categories [41]:

- Short-term (electromagnetic) transients
- Mid-term (electromechanical) transients
- Long-term transient

Figure 2.4 summarizes the phenomenon and control actions in the power systems based on its corresponding time-frame [42]. Lightning and switching events in power system take very less time compared to other categories, making it considered as short-term transient. Transient stability is considered as mid-term transient as it involves the electromechanical capability of the system. In addition, the measurement unit should be able to detect or measure the condition of the power system fast enough so that the system do not fail.

Power system simulation model could be differentiate into static and dynamic model where dynamic simulation helps in assessing stability and security of power systems. There are two model types of dynamic model: RMS and electromagnetic (EMT). RMS simulation is less time-consuming simulation compared to EMT making it more convenient for simulation of large power system. However, it may be insufficient to only conduct RMS simulation for dominant power electronics in the power system as RMS may be unsuitable for low system strength and unable to capture information for frequencies other than its fundamental [18].

The strength of a grid system can be described with short circuit ratio (SCR) shown in equation 2.2 [43].

$$SCR = \frac{S_{SC}}{P_R} \tag{2.2}$$

S_{SC} refers to the short circuit power level at the point of connection where the equipment with rated power P_R will be integrated to the grid. Weak grid, indicated with low SCR, becomes a concern as the control may not work properly (in stable manner), leading to sub-synchronous phenomenon and control interactions among neighboring power electronic devices. Thus, a low SCR means a high voltage sensitivity due to disturbance occur in the system [44].

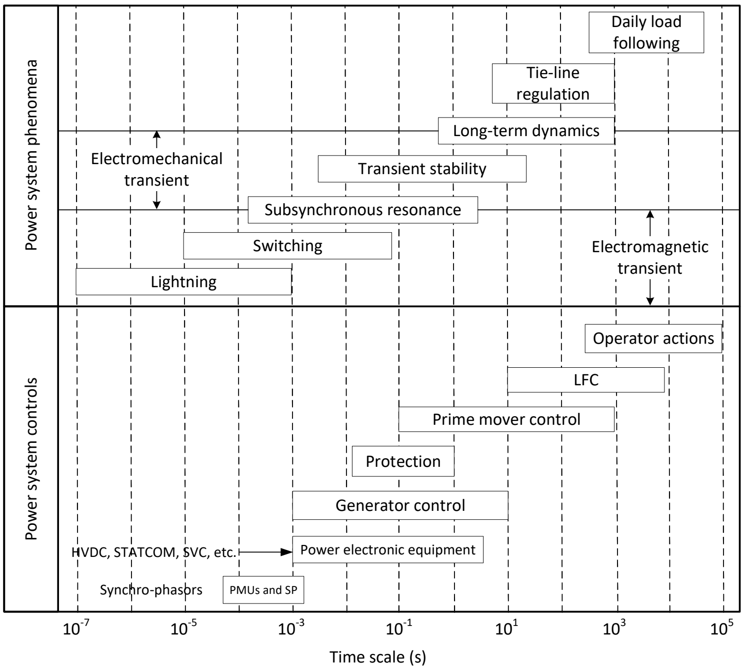

Figure 2.4: Time-frame classification for various transient phenomena

2.4 Conclusion

Electrolyzer and converter are the vital equipment of the PtX system to be connected to the electrical grid. There has been many studies and development on the equipments to have higher efficiency with also reducing the cost. This chapter presents the state-of-the-art of the most known electrolyzer technologies: alkaline, PEM, and SOEC electrolyzer. This chapter also discusses the converter that can be used for interfacing the electrolyzer to the grid system. Furthermore, the stability theory as the relevant topic of this study also be explained with a focus on the voltage stability.

Chapter 3

Modelling of Grid Test Study: IEEE 9-Bus System

This chapter describes the grid model used for studying the impact of the integration of PtX system in detail. The system is based on one of the benchmark power systems, known as IEEE 9-bus system, where it is modelled in PowerFactory simulation tool. Simulations of the base IEEE 9-bus system are also presented to show the response of the system before PtX integration. The simulation tests include the steady state and dynamic (RMS) simulation.

3.1 Model

Grid system enables power-generating plants to transmit electrical power to the loads through transmission and distribution lines. It consists of generators, transformers, transmission lines, and loads. As been mentioned before, the grid system studied for the project is IEEE 9-bus system.

PowerFactory has a built-in example of IEEE 9-bus system where the parameter settings are taken from [45, 46]. The built-in IEEE 9-bus system is adapted to be used as the study test in this project with some modification in the model. The single line diagram (SLD) of IEEE 9 bus system is shown in Figure 3.1.

Three synchronous generators (SGs) are connected to each corresponding transformer which also connected to the transmission system. There are 6 transmission lines in the IEEE 9-bus system with nominal voltage of 230 kV and nominal frequency of 60 Hz [46]. As in Europe and in particular, Denmark, the nominal frequency is 50 Hz, hence the nominal frequency of the system test is adjusted to be 50 Hz. Lastly, the IEEE 9-bus system has 3 loads connected to different buses at the system where the rated power of each load are different.

The type of buses in system is dependant on which equipment it is connected. There are 3 types of buses as the following [47, 48]:

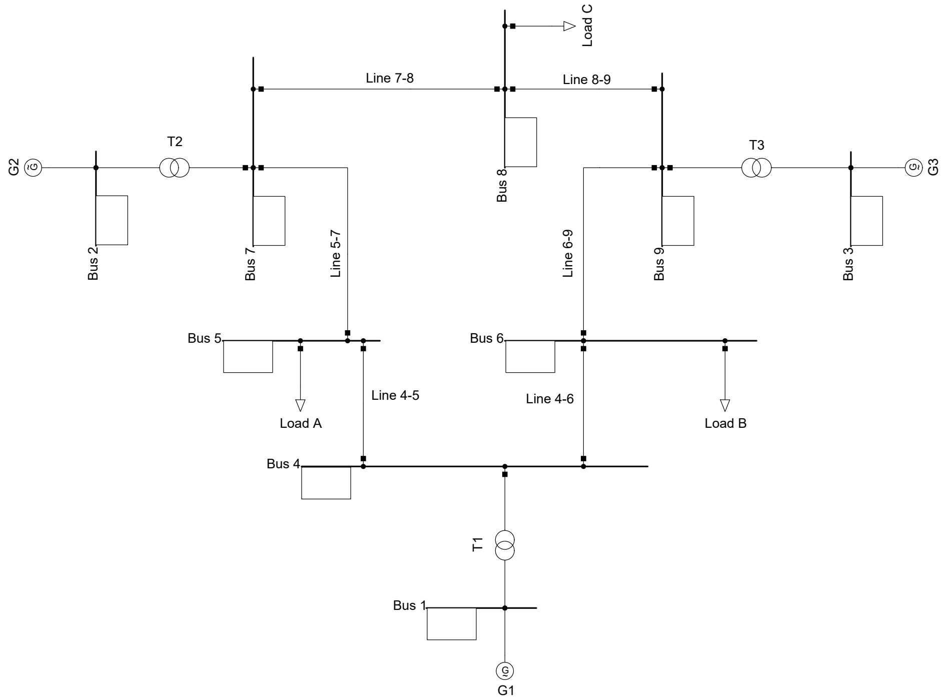

Figure 3.1: Single line diagram of 9-bus system

- **Load bus**, also known as PQ bus, is a term for bus that is connected to non-generator. The power at this type of bus is defined in the beginning and thus, the voltage and phase angle vary depending on the loading and network condition. In the deployed grid system, bus 5, bus 6, and bus 8 are considered PQ buses.

- **Voltage-controlled bus** or PV bus is bus which the voltage magnitude is controlled to be constant. If the bus is connected to generator, the output power can be controlled through its prime mover while the voltage is controlled through the generator excitation. This type of bus does not necessarily need to be connected the generator. It is possible to assign certain buses in which the voltage is controlled. Bus 2 and bus 3 are considered to be PV bus as it is connected to generator G2 and G3 respectively.

- **Slack bus** or swing bus is a bus designated to be the reference of other buses in the system. The variables taken as the reference for other buses from the slack bus are the voltage and phase angle with a value of 1 p.u. and 0° normally. Generator G1 of the IEEE 9-bus system is assigned to be the slack machine meaning that the bus connected to it, bus 1, is a slack bus.

3.1.1 Generator

SGs are placed in the IEEE 9-bus system with different rating for each power plant. From the built-in database of IEEE 9-bus system, generator G1 represents a hydro power plant while the other generators, G2 and G3, are coal power plants. However, to reflect more into the Danish grid system, all three SGs are assumed to be steam power plants. The modification of this is adjusted with the generator dynamic model. G1 operates with nominal voltage of 16.5 kV while G2 and G3 operate at 18 kV and 13.8 kV respectively. The rated power of G1 is 247.5 MVA, which is the highest compared to G2 and G3.

In a system, there should be at least one source serving as the reference where it provides the balance in power system [48]. This means that G1, as the slack machine, adjusts its output power depending on the supply and demand of power in the system. This is achieved by regulating its governor and excitation which corresponds to the active power and reactive power output of the generator. In the test study, G1 is set to generate voltage of $1\angle 0$ p.u. at bus 1.

In order to run the load flow simulation analysis, it requires the initial conditions of power and voltage magnitude and angle for each generator. Table 3.1 shows the initial conditions for each generator.

Table 3.1: Load flow initial conditions

Generator	V [p.u.]	δ [°]	P [MW]
G1	1.00	0	N.A
G2	1.025	N.A	163
G3	1.025	N.A	85

Aside from modelling the static model, it is also important to model the dynamic model of the SGs. This would enable the SGs to respond towards disturbances occurring in the grid. In case of fault condition, the power-generating plants should be able to withstand and support the grid to remain stable after the fault is cleared by reaching steady state condition. The control of the SGs may include the turbine-governor system, excitation system, power system stabilizers (PSS), etc.

Turbine-governor system

The modelling of turbine-governor system is important key in studying the the power system stability, especially related to the frequency and transient angle stability. Many types of turbine-governor system have been developed for different power plants. As been mentioned before, all SGs in the test system are considered to be coal power plants, the turbine-governor model can be used are TGOV1, IEEESO, and IEEEG1 [49]. This model could represent the steam turbine used in coal power plant.

It is recommended to use turbine-governor type IEEEG1 as it includes the rate limit of the valve control as well as the four steam-stages [49]. The block diagram of IEEEG1 is shown in Figure 3.2.

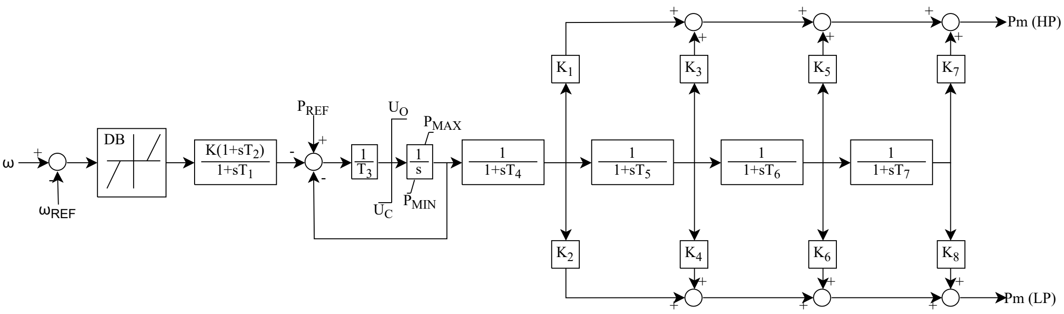

Figure 3.2: Block diagram of IEEEG1 steam turbine model

From the block diagram shown in 3.2, the model consists of the turbine section for high pressure (HP) and low pressure (LP). Physically, the steam goes into the HP section from the control valve and the inlet piping where the HP exhaust steam flows to the LP turbine. The control valve controls the steam flow through the turbine for load-frequency response. In case of change in the system causing the speed of the governor to increase/decrease, the control valve will control the speed by comparing the speed with its reference. However, this is only for normal speed/load control. For an overspeed condition, a dedicated overspeed control of the turbine is implemented to limit the speed and return to a steady state after disturbance [50].

PowerFactory has turbine-governor models including the IEEEG1 in its database, named "gov_IEEE_IEEEG1". This model is taken for the turbine-governor model in all 3 SGs deployed in the IEEE 9-bus system. The parameter setting is set as the standard values from PowerFactory. $K_1 - K_8$ represent the fraction of the mechanical power of HP and LP of the turbine. T_1 and T_2 are the time constants for the lag and lead of the steam controller and T_3 is the time constant of the valve position. $T_4 - T_7$ indicate the time constant for the steam inlet and 2nd, 3rd, and 4th boiler pass [49]. The outputs of the turbine are in the form of mechanical power, both for HP and LP section of the turbine.

Excitation system

An excitation system provides direct current to the field winding of the SG for maintaining the voltage at the terminal. This could result in the enhancement of the power system performance in regard to the stability where the control function includes the control of voltage and reactive power flow [50]. Modern excitation system should be capable to give instant response towards perturbation so that it could enhance the stability of the system.

The excitation system may include voltage transducer and load compensator, excitation control elements/regulator, exciter, and also power system stabilizer. The excitation system are classified based on the power source of the excitation: DC, AC, and static (ST) excitation system. In modern power system, most of the SGs employ the AC or ST excitation system [51]. The excitation system chosen to be implemented in the SGs under study is the ST excitation system. This type of excitation is powered with transformer or auxiliary generator windings and rectifiers [51].

A simple model of ST excitation system, named ST1A, is adapted in the SGs in the IEEE 9-bus system. The block diagram of the ST1A excitation system is shown in Figure 3.3.

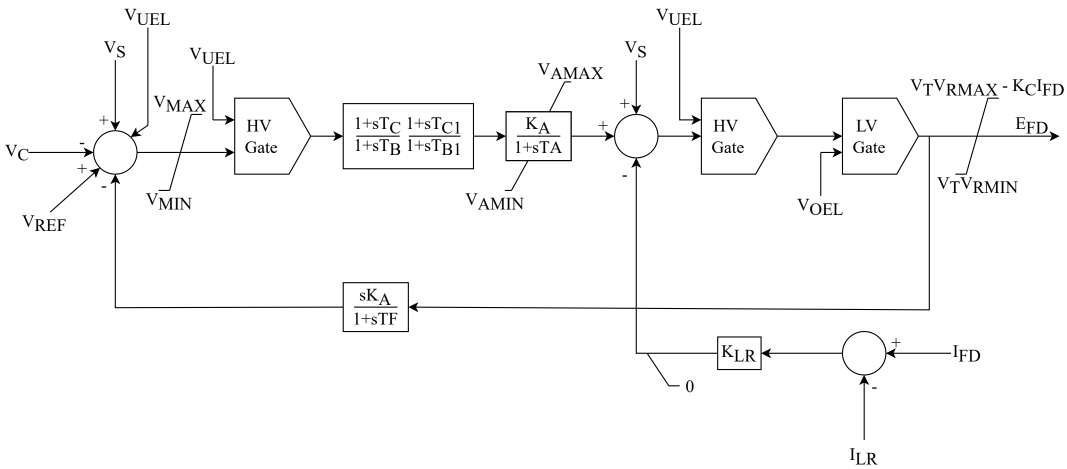

Figure 3.3: Block diagram of excitation type ST1A

ST1A is a potential-source controlled-rectifier excitation system where the rectifier regulates the excitation power supplied through a transformer from generator terminal or auxiliary bus. The inherent time constant of the exciter is very small which means that the excitation system may not require the exciter stabilization [50, 51]. This model offers a flexibility to reduce its transient either through its forward path from the time constant T_B and T_C or through its feedback function represented by K_F and T_F. The time constants T_{C1} and T_{B1} represent the transient gain while a simple gain, K_A, is used to show the relationship between the input and output of the rectifier. K_{LR} and I_{LR} define the limiter function of the field current to protect the generator rotor and its exciter.

ST1A model has been defined in the database of PowerFactory including its parameter setting under the name of "exc_IEEE_ST1A". This standard value is adapted and implemented in all the 3 SGs in the IEEE 9-bus system.

A voltage transducer and load compensator has to be modelled to give input V_C

to the excitation system. Dedicated block diagram of voltage transducer and load compensation can be found in the library of PowerFactory, named "vtc_IEEE_1". The equation represents this model is shown in eq. 3.1.

$$V_C = |V_T + R_C X_C I_T| \frac{1}{1 + sT_R} \tag{3.1}$$

As no load compensation is considered in the system, the R_C and X_C is set to be zero. In general, the time constants T_R of the transducer is relatively small and thus it can be assumed to be zero [51]. This results in the input voltage to the excitation system, V_C, equals to the measured voltage at the terminal.

Power system stabilizers

A PSS might be included in the excitation system to improve the performance of the power system by damping the oscillation occurring due to disturbance through its excitation control [51]. A simple model of PSS known as PSS1A is implemented in this project for all 3 SGs where this model can be found in the PowerFactory library, named "pss_IEEE_PSS1A". Figure 3.4 shows the block diagram of the model where the parameter setting of the PSS implemented in the project is based on the values from the standard in PowerFactory.

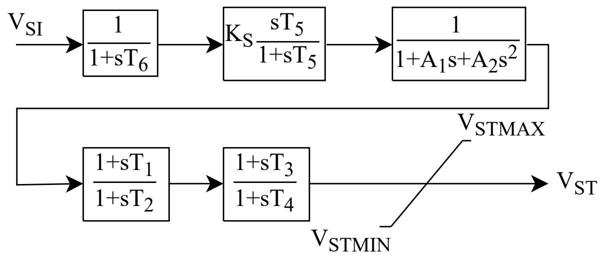

Figure 3.4: Block diagram of PSS type PSS1A

The input signal of the PSS can be speed, frequency, and power, which is denoted as V_{SI}. The time constant of the PSS is represented by T_6 while the gain is determined by K_S with a time constant of T_5 for the signal washout. Implementing A_1 and A_2 would take the low-frequency effects of high-frequency torsional filters into account. However, as this is not necessary in the study for this project, these two parameters are set to be zero. This model also includes two-stages lead-lag compensation, with time constants of T_1 to T_4. Lastly, the ouput of the PSS, denoted as V_{ST} is limited with a limiter. V_{ST} becomes an input to the excitation system, V_S.

3.1.2 Transformer

In PowerFactory, the IEEE 9-bus system is also equipped with transformers connecting the transmission system to each SG. The transformer models used for the study project are taken the same as with the examples from the IEEE 9-bus system in PowerFactory. Each transformer has different rated power and nominal voltage depending on the SG connected to the transformer. The connection for each transformer is YnD5 meaning that the HV-side of the transformer has Yn configuration while the LV-side has delta configuration with a phase different of 5·30° = 150 °.

The transformers are modelled as ideal transformers where the voltage-current relation is linear (no saturation) and no losses due to magnetisation. The leakage impedance is equally distributed for both HV- and LV-side of the transformers. Table 3.2 summarizes the specifications of each transformer deployed in the system.

Table 3.2: Transformer specification of IEEE 9-bus system

Parameter	T1	T2	T3
S_{Rated} [MVA]	250	200	150
HV_{Rated} [kV]	230	230	230
LV_{Rated} [kV]	16.5	18	13.8
Vector group	YnD5	YnD5	YnD5
Reactance X_1 [p.u.]	0.144	0.125	0.0879
Resistance R_1 [p.u.]	0	0	0
Tap position	0	0	0

3.1.3 Transmission line

Transmission line can be modelled as lumped (π) or distributed model. From the benchmark IEEE 9-bus system in PowerFactory, the transmission lines are considered as π-model where each line has different impedance and susceptance specified in per km. The transmission lines are modelled as overhead line meaning it is bare conductor without insulation. The conductor material is aluminium with rated voltage and current of 230 kV and 1 kA respectively.

The zero sequence of the impedance and susceptance of all transmission lines is set to be 0 and the negative sequence is the same as the positive sequence. The transmission line could operate with maximum temperature of 80°C. Table 3.3 summarizes the specification data of the transmission lines used in the project study. The resistance data shown in the Table 3.3 is under the temperature condition of 20°C.

The numbering of transmission line means that the transmission line connects bus x to bus y i.e. Transmission line 5 - 7 means that bus 5 and bus 7 are linked through that line.

Table 3.3: Transmission line specification of IEEE 9-bus system

Parameter	Transmission line					
	4 -5	4 - 6	5 - 7	6 - 9	7 - 8	8 - 9
Type	OHL	OHL	OHL	OHL	OHL	OHL
Material	AL	AL	AL	AL	AL	AL
V_{rated} [kV]	230	230	230	230	230	230
I_{rated} [kA]	1	1	1	1	1	1
Length [km]	1	1	1	1	1	1
Resistance R′ [Ω/km]	5.29	8.993	16.928	20.631	4.4965	6.2951
Reactance X′ [Ω/km]	44.965	48.668	85.169	89.93	38.088	53.3232
Susceptance B′ [μS/km]	332.7	298.69	578.45	676.75	281.66	395.08

3.1.4 Load

Load can be classified into three categories: constant current, constant impedance, and constant power [47]. In the load modelling in PowerFactory, general load model are taken where these loads are balance loads. From the benchmark model of IEEE 9-bus system, there are three loads existed in the system. The loads are modelled to have constant active and reactive power demand and these loads are independent to the voltage [46]. The load data is summarized in Table 3.4.

Table 3.4: Load data of IEEE 9-bus system

Load	Connected to	P [MW]	Q [MVAr]
Load A	Bus 5	125	50
Load B	Bus 6	90	30
Load C	Bus 8	100	35

Load flow calculation determines the initial condition for dynamic simulation in PowerFactory. During the dynamic simulation, the loads are considered to be equivalent as impedance [46].

3.2 System response

The existed model of IEEE 9-bus system with some adjustification of the dynamic model is simulated to show the result is according to what is expected. This validation include the load flow calculation and also the RMS simulation to enable showing the result.

3.2.1 Load flow under normal condition

Load flow calculation is done to show the power flow from the SGs to the loads and this can show the losses in the system. The calculation for the load flow simulation by considering balance condition in the system.

The loads consume 315 MW and 115 MVAr in total which is in line with the load data specified in Table 3.4. There is losses of 4.79 MW and -87.28 MVAr in the transmission lines and also the transformers. Hence, the SGs should be able to supply power, both active and reactive, to cover the demand from the loads and also the losses in the grid. It can be seen that the SGs have reserve power of 199.71 MW meaning that these SGs can increase the power generation in case of the increase of demand.

It is noted that G1 adjust its production, as can be seen in the initialisation in Table 3.1, that G1 is the reference machine. It produces 71.8 MW where this generator regulates the voltage at the generator terminal to be $1\angle 0$ p.u. Table 3.5 shows the voltage magnitude and the phase angle at each bus during normal operation.

Table 3.5: Voltage profile of IEEE 9-bus system under normal operation

Bus	u, magnitude [p.u.]	u, angle [deg]
Bus 1	1.000	0.0
Bus 2	1.025	9.0
Bus 3	1.025	4.3
Bus 4	0.995	147.6
Bus 5	0.972	145.7
Bus 6	0.989	146.0
Bus 7	1.019	153.4
Bus 8	1.009	150.4
Bus 9	1.026	151.6

Bus 2 and Bus 3 have voltage magnitude of 1.025 p.u. This is due to the setting of the generators connected to the buses. G2 and G3 are set to control its terminal voltage level to be constant. The active power supplied by these SGs is also set to be constant. Thus, the SGs adjust their reactive power supply so that it could maintain the voltage terminal as wanted.

Overall, the result shows that there is no over- and under-voltage condition occurring during normal operation. The loading of each component in each component of the IEEE 9-bus system is also not violated as it is not overloaded.

3.2.2 Short-circuit calculation

The short-circuit level is calculated to see the short-circuit power at each bus of IEEE 9-bus system containing the specified SGs. From the calculation of short-circuit power, it determines how strong the grid system is. The method of calculating the short circuit is based on IEC 60909. Table 3.6 shows the short-circuit power in MVA for each bus of the system.

Table 3.6: Short-circuit power of IEEE 9-bus system

Bus	Short-circuit power [MVA]
Bus 1	1629.3
Bus 2	1488.7
Bus 3	1156.0
Bus 4	1216.2
Bus 5	898.7
Bus 6	855.0
Bus 7	1227.4
Bus 8	978.2
Bus 9	1104.2

The result shows that the short-circuit power is higher if it is closer to the generator and the highest short-circuit power is at the generator terminal with the highest rating power. This calculation helps in determining which bus will be connected to the PtX system.

3.2.3 RMS simulation

The RMS simulation is run to obtain the response of the system of pre-fault, during fault, and after fault condition. The model is run by injecting symmetrical 3-phase short-circuit fault at the middle of transmission line 6-9. The fault impedance is assumed to be 1mΩ resulting in large voltage dips. During pre-fault condition, the system should be in steady state condition. The fault is cleared at 100ms after the fault injected as stated in [52]. In the simulation, The 3-phase fault is injected at 30s and cleared at 30.1s. This is done by opening the circuit breaker at both end of the transmission line. The RMS simulation is run under balance condition with a step size of 10ms. Figure 3.5 and Figure 3.6 depict the response of one of the SGs in the system towards the occurrence of a fault.

Figure 3.5 shows the frequency and voltage measurement at bus 6. It can be seen that the voltage and frequency are steady before the fault injection. The pre-fault voltage profile also match with the load flow calculation shown in Table 3.5. During the fault condition, voltage dip occurs due to the low fault impedance while the frequency measured increases as the effect of fault occurrence. After the

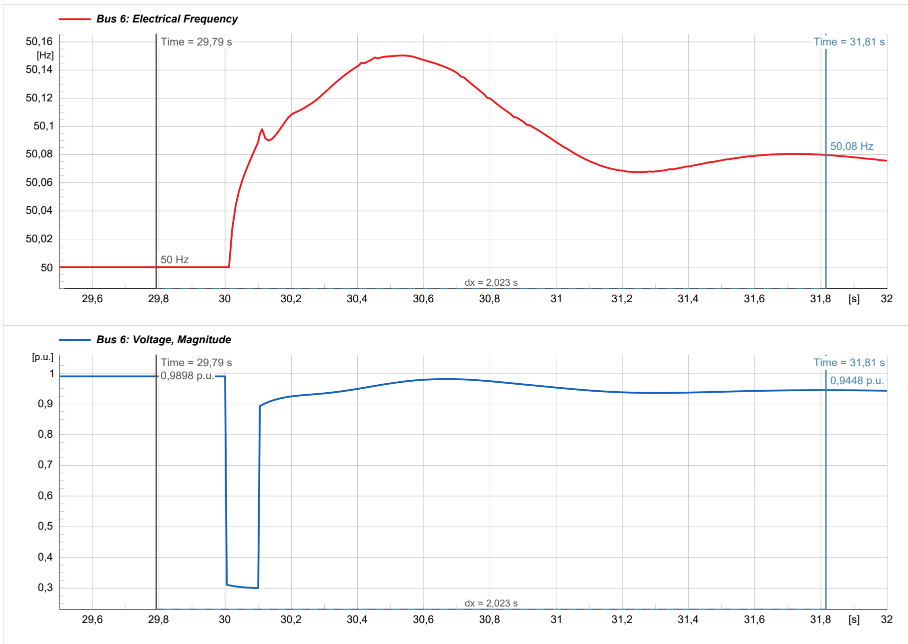

Figure 3.5: Response of the system on the frequency and voltage due to fault injection

fault clearance, the system tries to reach new steady-state point. The new voltage level reached after the fault is cleared is lower than the pre-fault because there is a change in the power flow. This is due to the opening of the circuit breaker for both side of the transmission line, meaning that the faulted-line is removed from the system. On the other hand, the frequency measured after fault is higher compared to the pre-fault condition as there is loss of line in the system.

Before the fault injected, the SGs supply power to the load as initiated. This is reflected in the result shown in Figure 3.6 which is showing the response of G1. At pre-fault condition, its speed is 1 p.u. and supplying active and reactive power of 71.8 MW and 10 MVAr. This is equal to the result obtained in the load flow calculation. It is also the same for the steady state point for the mechanical torque. This can be validated by using eq. 3.2.

$$\tau_{mech} = \frac{P_{mech}}{\omega} \tag{3.2}$$

Mechanical torque, τ_{mech}, is the ratio between the mechanical power of the generator, P_{mech}, to the rotor speed. In steady state, the actual rotor speed equals to the rated speed of the generator. This means that the mechanical torque is the ratio of the actual power generated to the rated power of the generator. This gives τ_{mech} of 0.29 p.u. at pre-fault condition.

During fault condition, the speed of the generator increase vastly while the torque drops. As the turbine-governor model of the generator has been imple-

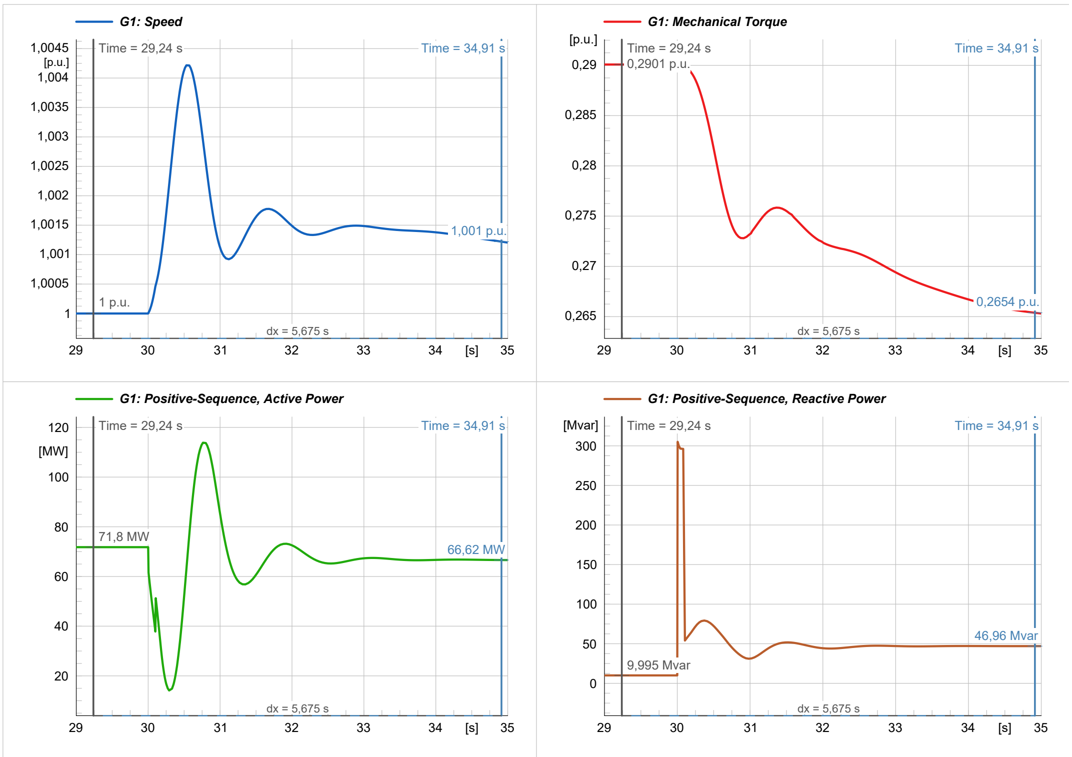

Figure 3.6: Response of G1 due to fault injection

mented, it controls the generator speed by comparing it with the reference speed so that it could reach new steady state condition after the fault is cleared.

The active and reactive power oscillates during the fault and these reach steady state after the clearance of fault with the help excitation system. The PSS helps in damping the power swing and achieve steady state faster compared to without PSS implemented. This result also reflected in the voltage measurement in Figure 3.5 where the oscillation of the voltage is damped rapidly.

3.3 Conclusion

This chapter shows the model implementation of IEEE 9-bus system used for the study project. The simulation shows that the model works properly as the it yields the same result for the load flow calculation and RMS simulation at pre-fault condition. The response of the system is shown where the system could control the governor of the generator based on the speed and with the help of excitation system and PSS, the system is able to reduce the impact of the fault and damp the oscillation faster to reach steady-state condition quicker.

Chapter 4

Modelling of Power-to-X

This chapter discusses the modelling of PtX in PowerFactory. The PtX model capability is described in this chapter. Following this, the dynamic model representing the PtX is explained in detail i.e. the control strategy of the PtX model. Lastly, validation of the PtX model is presented at the end of this chapter.

4.1 Base model

PtX is represented by converter model in PowerFactory where the parameter setting of the power converter in this project is dedicated for an electrolyzer converter. PEM electrolyzer technology is used as the benchmark for modelling the electrolyzer converter model in the simulation. Silyzer 300, one of the electrolyzers from Siemens Energy has rated power of 17.5 MW [33]. The rated power of the converter model is assumed to be the same as the electrolyzer. In order to compare the impact of the PtX integration to the system with before the integration, the PtX is integrated to the IEEE 9-bus system to substitute one of the existing loads in the system.

In determining which load should be substituted by PtX, the SCR is first determined to know which bus of the system are the weakest part of the grid. Using eq. 2.2 and the result of short-circuit calculation shown in Table 3.6, the lowest SCR obtained is at bus 6. Thus, the PtX is integrated at bus 6 to substitute the existing load connected to this bus.

Bus 6 originally is connected to load B, which consumes 90 MW. To substitute this load, the PtX is set to consume 90 MW. As the benchmark model of PtX is assummed to have rated power of 17.5 MW, the model is defined to be aggregated so that it could supply 90 MW at the point of connection. This is achieved by increasing the capability of the model to be 105 MVA (6 sets of 17.5 MW electrolyzer).

From the information obtained from Siemens Energy as shown in **??** in Appendix A, the PQ capability of the electrolyzer could operate with power factor

> 0.95. This PQ capability is set to be the limiter of the operation of the model developed in the simulation.

4.2 Dynamic model

Dynamic model of the converter is used to represent the behaviour of the converter's controllers for dynamic simulation. The control strategy used to model the converter is based on the grid following converter as described in [53]. The converter is controlled using current control mode to generate active and reactive power by taking the synchronized phase from the grid where this strategy can help in regulating the bus voltage and frequency.

Figure shows the frame of the converter's dynamic model implemented in PowerFactory.

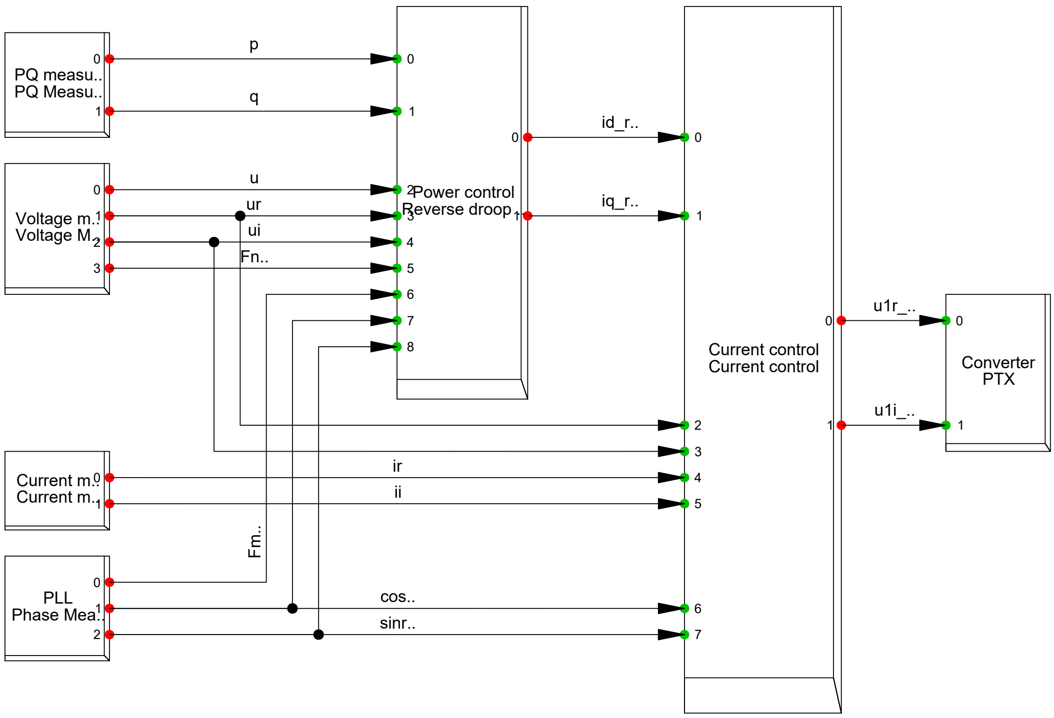

Figure 4.1: Dynamic model of PtX in PowerFactory

The dynamic model consists of measurement devices, reverse droop control, and current control. The output of the controller is the voltage, real and imaginary part where these signals becomes the input of the converter.

4.2.1 Reverse droop control

Current control mode used by grid following converter regulates the active and reactive power through its inner current loop. Droop control cannot be applied for grid following converter as the output of this control is the voltage and frequency. Instead, reverse droop control can be implemented to regulate the bus frequency and voltage. The relationship of the active power-frequency and reactive power-voltage can be described with eq. 4.1 and eq. 4.2.

$$P^* = \frac{1}{m_r}(\omega^* - \omega_g) \tag{4.1}$$

$$Q^* = \frac{1}{n_r}(E^* - E_g) \tag{4.2}$$

The measured frequency and voltage are denoted with ω_g and E_g and the reverse droop characteristic by m_r and n_r. The reverse droop control maintains the voltage and frequency by comparing the measurement to its reference.

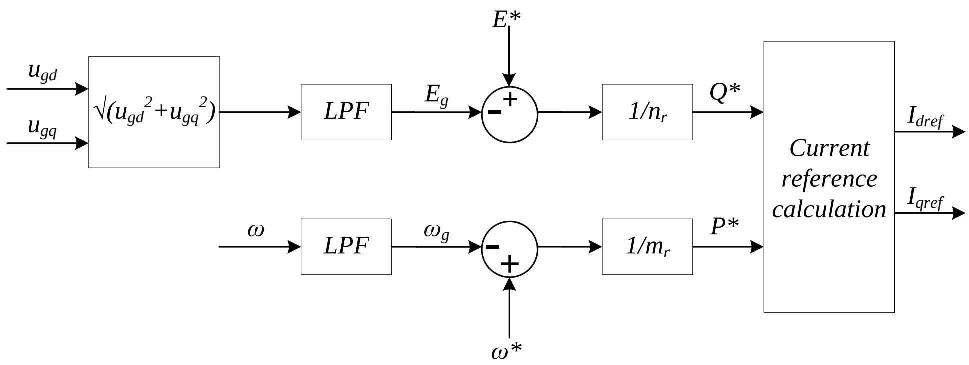

Figure 4.2: Reverse droop control block diagram

The block diagram of reverse droop control is shown in Figure 4.2. It shows that the measurement of the voltage and phase are sent to low pass filter (LPF) block. The LPF determines the bandwidth of the loop control. The output of the LPF then compared to the voltage and phase reference. The difference between the measurement and the reference are taken to calculate the power reference by multiplying the difference with the droop characteristic. The calculated power references, P^* and Q^*, are used to determine the current reference i_{dref} and i_{qref} by using eq. 4.3 and eq. 4.4. The output of reverse droop control is delivered to the inner current loop control.

$$i_{dref} = \frac{u_{gd} \cdot P^* + u_{gq} \cdot Q^*}{\sqrt{{u_{gd}}^2 + {u_{gq}}^2}} \tag{4.3}$$

$$i_{qref} = \frac{u_{gq} \cdot P^* - u_{gd} \cdot Q^*}{\sqrt{{u_{gd}}^2 + {u_{gq}}^2}} \tag{4.4}$$

The implementation of the reverse droop control in PowerFactory is shown in Figure 4.3. The inputs of the implemented reverse droop control model are the active and reactive power measured, real and imaginary part of the voltage, the nominal voltage, phase angle in term of cosϕ and sinϕ, and the nominal frequency.

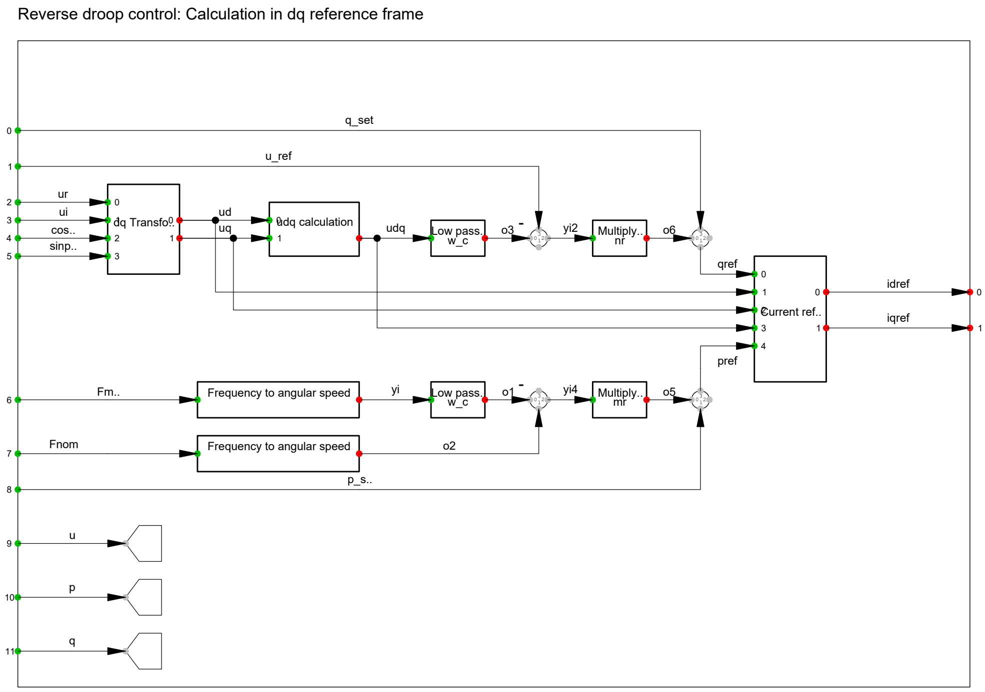

Figure 4.3: Implementation of reverse droop control in PF

The PQ measurement is used to be the power setpoint during the dynamic simulation. If this is not set beforehand then the PtX model will not consume any power initially. The nominal voltage and frequency are set to be the reference of the calculation. As the calculation is done in dq-reference frame, the measured voltage has to be transformed into dq-frame. Eq. 4.7 and eq. 4.8 transform the real and imaginary part of the voltage into dq-frame with the help of cosϕ and sinϕ.

$$u_d = u_r \cdot cos\phi + u_i \cdot sin\phi \tag{4.5}$$

$$u_q = -u_r \cdot sin\phi + u_i \cdot cos\phi \tag{4.6}$$

The model also has the electrical frequency of the grid as an input variable. The frequency measured is used for calculating the difference in frequency between its nominal. Thus, the model can regulate its active power output based on the frequency deviation. The parameter setting of the reverse droop control is listed in Table B.1 in Appendix B. The droop characteristic is adjusted to be in the range determined by the system operator as stated in [27] and the corner frequency parameter of the LPF is taken from [54].

4.2.2 Current control

The innerloop control is intended to regulate the output power of the converter. The block diagram of the current control is shown in Figure 4.4.

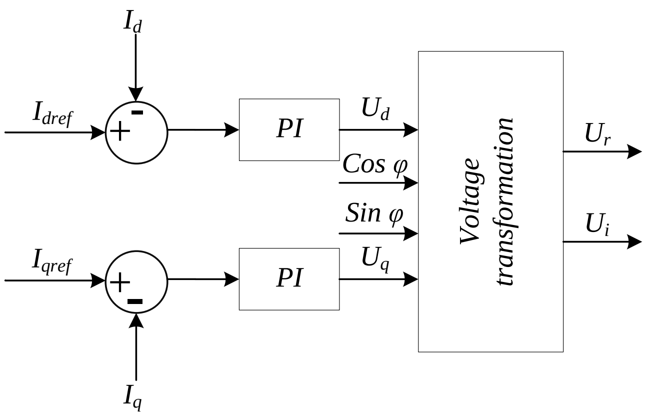

Figure 4.4: Current control block diagram

The innerloop control model calculate the difference between the current reference with the measured current, where the calculation is in dq-frame. By deploying PI controller, the model could obtain the voltage value.

The implemented current control in PowerFactory is shown in Figure 4.5. The model inputs are the current reference i_{dref} and i_{qref} from the reverse droop control, the real and imaginary part of the measured current, and cosϕ and sinϕ.

The current control model transform the input current measured into dq-frame so that this measured current could be subtracted from the reference current. To transform the current from real and imaginary into dq-frame, eq. 4.7 and eq. 4.8 are applied, which are the same way for transforming the voltage described in reverse droop control.

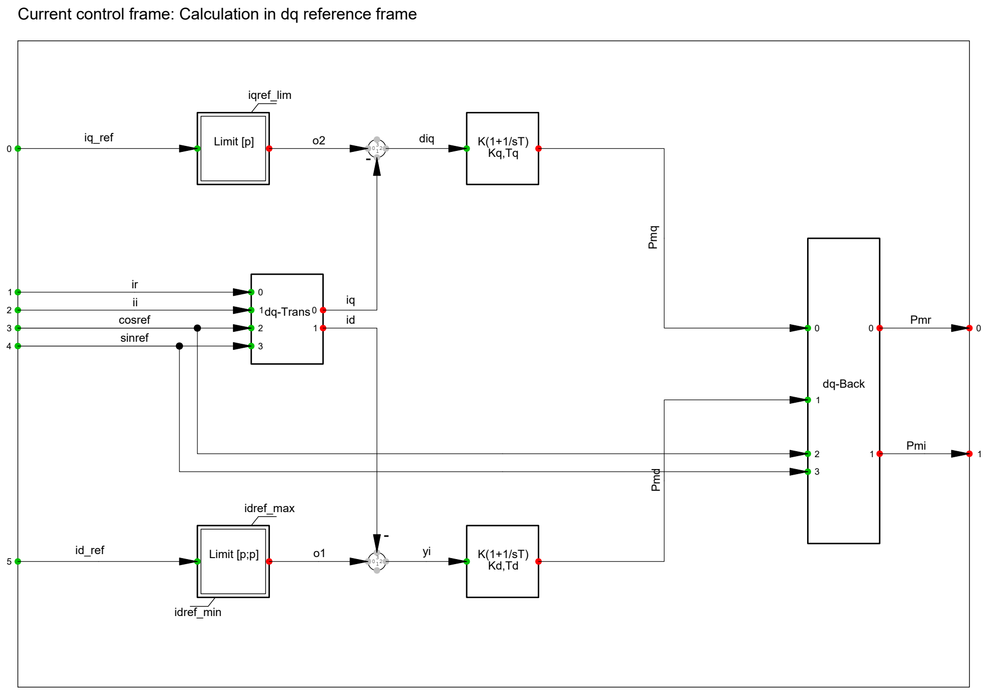

Figure 4.5: Implementation of current control in PF

$$i_d = i_r \cdot cos\phi + i_i \cdot sin\phi \tag{4.7}$$

$$i_q = -i_r \cdot sin\phi + i_i \cdot cos\phi \tag{4.8}$$

As the electrolyzer modelled is based on PEM technology, the elecrrolyzer should not be able to supply active power to the grid. This can be set by putting limiter to the i_{dref}. The current reference i_{qref} is also subjected to a limiter to limit the reactive power output where the PtX model could operate by supplying/consuming reactive power of 0.312 p.u. from its rated power. The difference of the current reference and the measured current is applied to the PI controller to gain the voltage. The calculated voltage is transformed back to real and imaginary part to give input to the converter model. The parameter setting of the current control is listed in Table C.1 in Appendix B where the PI controller is adjusted according the report from [54].

4.2.3 Measurement devices

There are four measurement devices implemented to give input to the controllers of the PtX model: PQ measurement, voltage measurement, current measurement, and phase-locked loop (PLL). All measurement devices measure their variables at the terminal of the converter connection to the corresponding bus. The unit of the measured power is in MW and MVAr where these parameters are set to be the power setpoint.

The voltage measurement measures the voltage at the point of connection. Three variables of voltage are taken to be used in the calculation, the total voltage u and its real and imaginary part of the voltage, u_r and u_i. The measure voltage unit is in p.u. of its nominal voltage. Besides, the voltage measurement in PowerFactory is able to measure the nominal grid frequency, denoted F_{nom}. This paramater is used for setting up the frequency reference. The nominal frequency has a unit of Hertz.

Current measured from the terminal is composed of real and imaginary part of the current, i_r and i_i respectively. These variables are used to be the input of the innercurrent loop. The implementation of PLL is to measure the phase angle where the variables considered are cosϕ and sinϕ. Also, the PLL can measure the the electrical frequency, denoted F_{meas}. Frequency F_{meas} is different from F_{nom} as F_{meas} is used to measure the frequency of the system over time. This means that F_{meas} value can change if the system is subjected to disturbances. The measurement of F_{meas} is in Hertz.

4.3 Conclusion

This chapter describes the modelling of the PtX model in PowerFactory both for its static and dynamic model. The PtX is defined to be aggregated so that it has rating power of 105MVA and could operate to power factor of 0.95. Later, the dynamic model of the PtX is explained where it consists of the measurement devices, reverse droop control, and current control. The objective of this control is for the implemented model could regulate its power based on reverse droop control strategy.

Chapter 5

Impact of Power-to-X integration to the system

This chapter discusses the impact of the integration of PtX in the IEEE 9-bus system. Several simulation cases are simulated to observe the response of the PtX and also the system when disturbances occur in the system. This chapter also shows the response of the system if one of the SGs is replaced with wind turbine generator (WTG).

5.1 PtX integration in IEEE 9-bus system

As been explained in Chapter 3, the PtX model is defined to have rated power of 105 MVA. The PtX under normal condition is set to consume 90 MW at the point of connection, which is at bus 6. This is to match the replaced existing load B connected to bus 6 where load B consumes 90 MW and 30 MVAr. PtX is assumed to only consume active power under normal condition. To be able to compare the result between before and after the integration of PtX, load B power consumption is adjusted to only consume active power with the same amount as PtX.

Several simulations are performed to investigate the impact of PtX integration in the system, such as fault and loss of generation. The fault simulations are varied depending on the type of fault and the fault location. The fault impedance considered for all simulations is1 mΩ The following sections describe the simulations obtained for each simulation scheme.

5.2 Study test 1: Symmetrical fault at the middle of transmission line 6-9

A symmetrical fault is injected at the middle of transmission line 6-9 where the fault is cleared at 100ms after the fault injected. The fault is cleared by opening the breaker at both end of the transmission line 6-9. The response of the PtX due to symmetrical fault is shown in Figure 5.1.

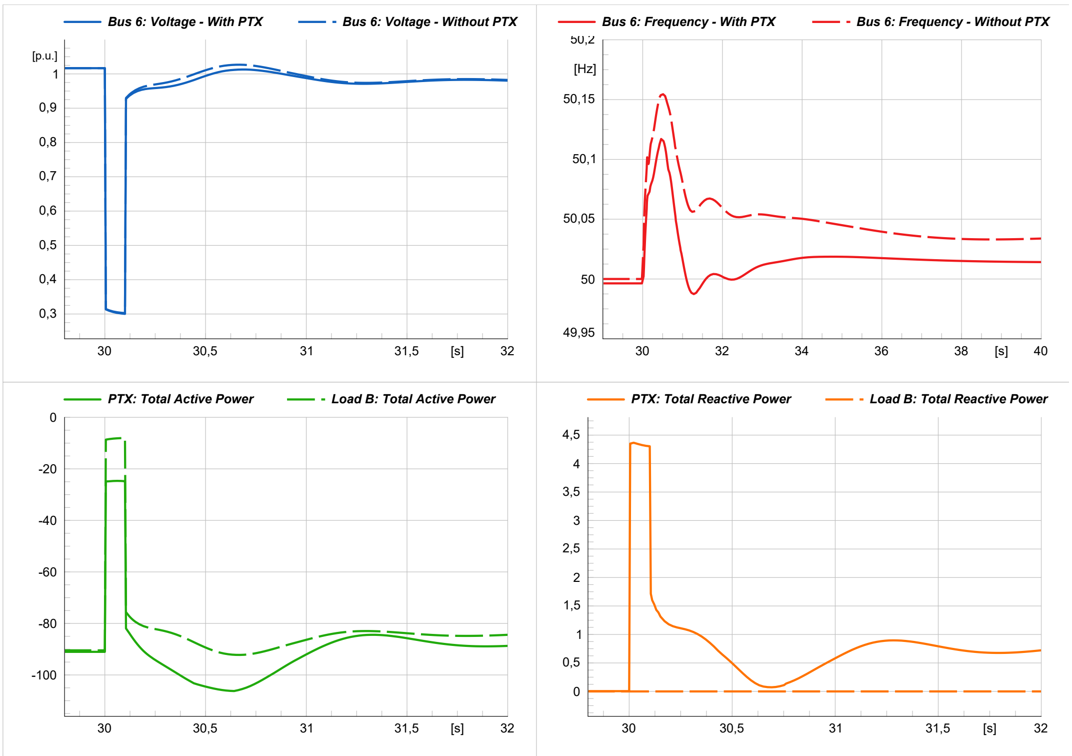

Figure 5.1: PtX response towards symmetrical fault

The response of the PtX model is compared with the response of the replaced load B at bus 6 (before PtX integration) as shown in Figure 5.1. The PtX model reduces its active power consumption due to the fault occurring in the line. The PtX model provides active power reduction when the fault occurs with a slope lower than the load. The Ptx model is also able to provide reactive power during the fault occurrence. Due to the provision of active and reactive power control from the PtX model, this affect the voltage and the frequency response of the system.

The voltage behaviour is similar to before the integration of PtX. However, it can still be seen that the voltage is more damped after the fault is cleared for the simulation with PtX integrated. The frequency measured is also showing similar response. The frequency deviates due to the fault occurrence in the system. But the

PtX helps in keeping the frequency to not deviate as large as without the control of the PtX. Hence, the frequency reaches its steady state faster compared to without PtX implementation.

As PtX model gives an impact to the system, the dynamic of the system is also changed reflected by the response of the SGs connected in the IEEE 9-bus system. Figure 5.2 shows the response of G1 towards the symmetrical fault.

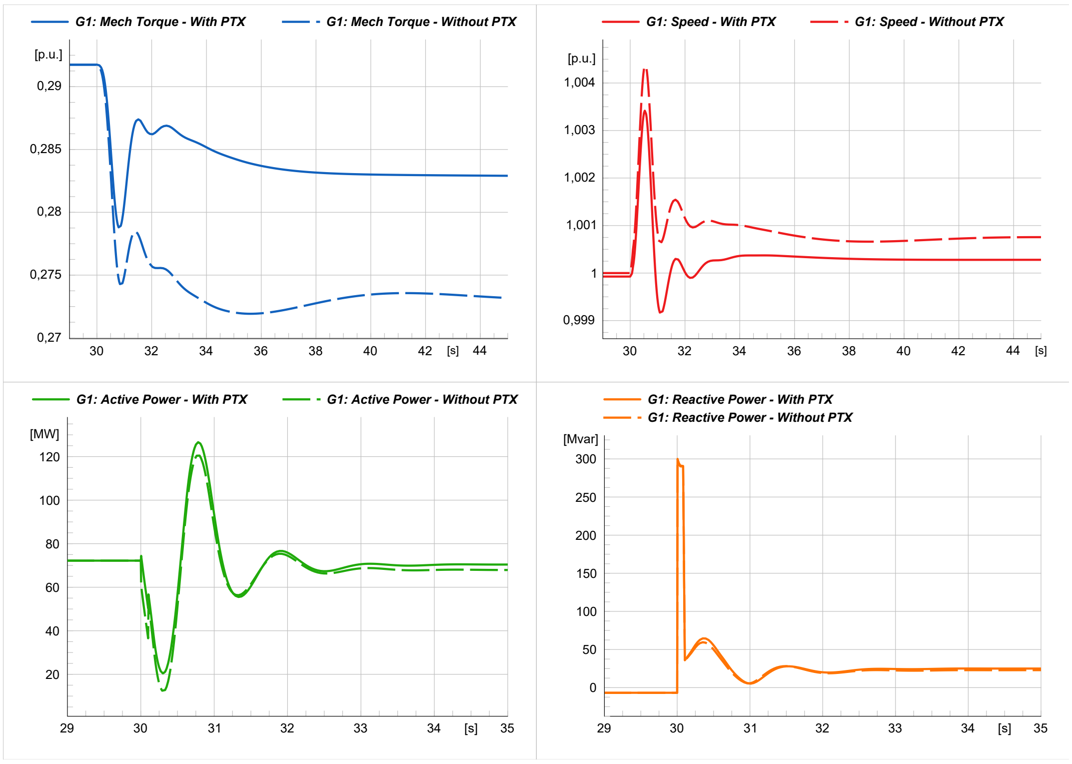

Figure 5.2: G1 response towards symmetrical fault

The active and reactive power out G1 are relatively similar for with and without PtX model in the system. G1 reduces its generation during the fault condition as the demand of active power is reduced. On the other hand, the reactive power is increased drastically during the fault. This happens as the response of G1 to support the grid voltage. After the fault is cleared, the power output oscillates for a moment before reaching steady state. The mechanical torque and speed variables of G1 are different for simulation with PtX and without PtX implemented. As the implemented model of PtX is able to provide power regulation, the deviation in the mechanical torque and speed are smaller compared to without PtX. This result shows that the PtX contributes to maintain the stability of the system by regulating its power output.

5.3 Study test 2: Loss of generator

One of the SGs in the IEEE 9-bus system is simulated to be disconnected to show the response of the implemented PtX towards sudden loss of generation unit. The 1040
SG that is simulated to be disconnected is G3. Figure 5.3 shows the response of the PtX compared to result with load B existed in the point of connection.

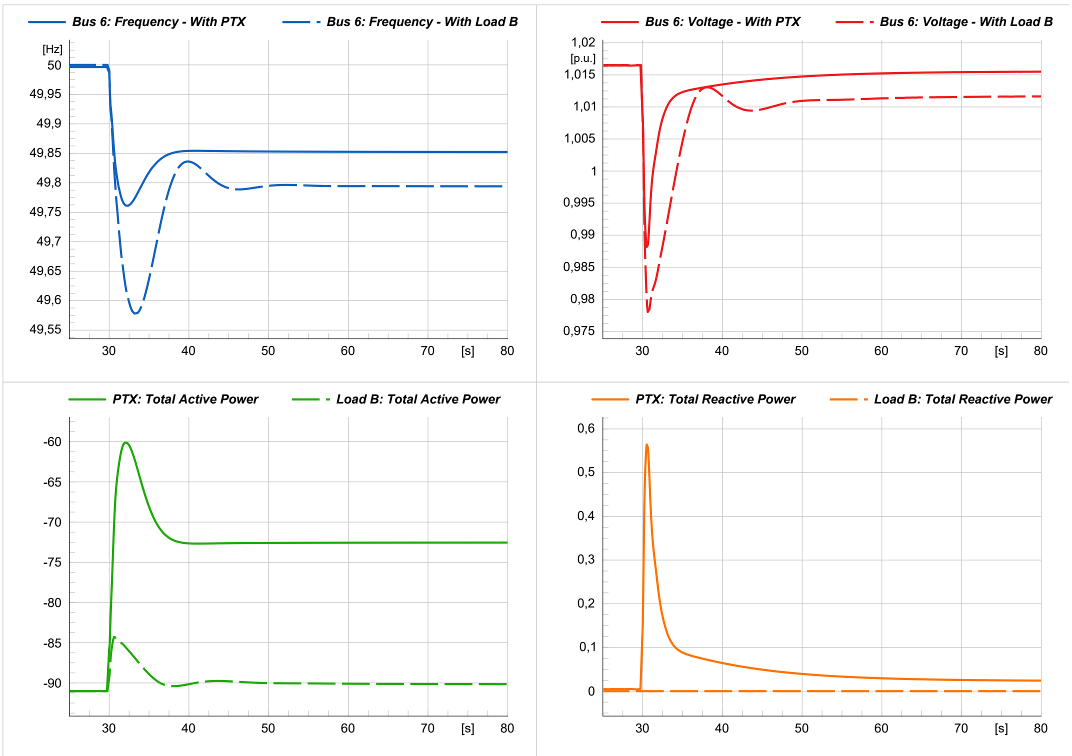

Figure 5.3: PtX response towards loss of generation

Due to sudden loss of G3, the frequency, mainly, and the voltage are affected. To help in stabilizing the frequency and voltage to not deviate too large from its normal pre-fault condition, the PtX reduces its active power consumption and supply reactive power to the grid. 1045 This results in the system frequency to not drop so large as without PtX where the frequency reaches the new steady state faster. Similar result is also observed for the voltage measurement where the implementation of the PtX improve the voltage performance on the system. The voltage profile is close to its pre-fault condition with PtX integrated in the system as the model 1050 could supply reactive power to the grid while the load is not controlled to provide this functionality.

PtX integration affects the response of the system towards the loss of generation unit G3. Figure 5.4 shows the response of one of the SGs, G1, towards the loss of generation for simulation with PtX and without PtX.

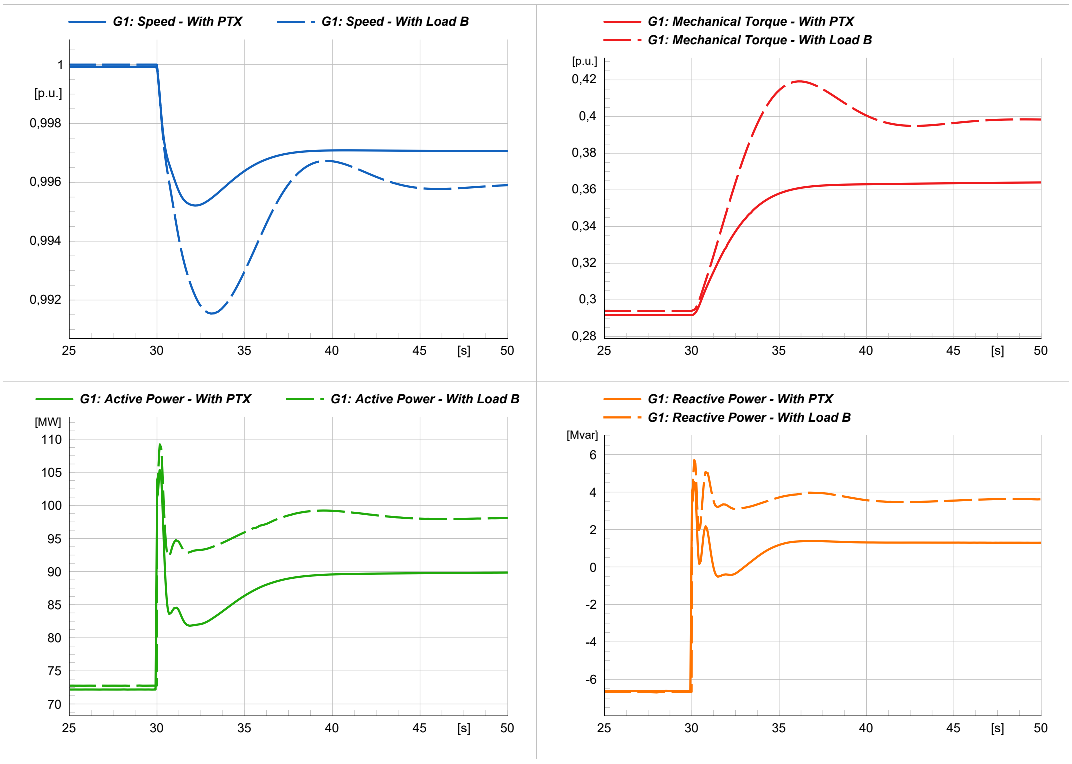

Figure 5.4: G1 response towards loss of generation

The result shows that G1 increases its power generation both for active and reactive power as the response due to the loss of generation. However, the increase of power is not as high if the PtX is not implemented. This is because the PtX lower its power consumption and the power comsumption by PtX is lowered larger than without PtX. This result is also reflected on the speed and torque of the generator where the speed of the generator decreases resulting in the increase in the torque.

5.4 Study test 3: Minimal operating load

This simulation is intended to show the response of the developed PtX model if it operates at its minimum operating load where the fault type simulated in this simulation is symmetrical fault. From table 2.1, it is assumed that the minimum loading of the developed is 10% of its rated power. Thus the initial condition of the simulation is adjusted so that the PtX operates at the minimum loading. The result of this simulation is compared with PtX operates at its normal condition as been simulated in the previous cases. Figure 5.5 shows the result of the simulation for PtX model operates at its minimum loading where the transmission line 6-9 is subjected towards symmetrical fault at the middle of the line.

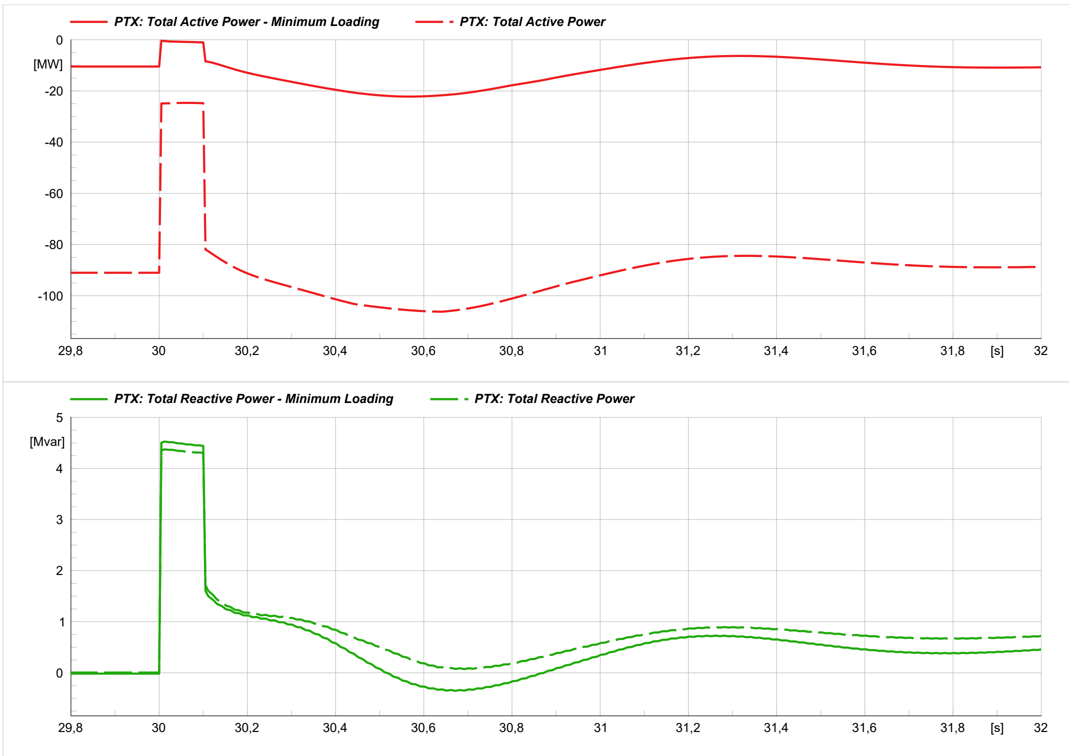

Figure 5.5: PtX operates at its minimum loading

The result shows similar behaviour of the active and reactive power response when symmetrical fault occurs at the line. The differences lies in the slope of active power consumption. When the PtX operates at its lower consumption, its capability to reduce the power consumption is limited. This is caused by the limiter implemented in the controller. This is to reflect the physical capability of PEM electrolyzer as this technology cannot supply active power to the grid. The reactive power values for both simulations, minimum loading and normal condition, yields similar result as the initial condition for both condition are the same. The grid response shows similar behaviour where the differences are in the magnitude of the values. This is due to the difference in power consumption between the two simulation conditions.

5.5 Study test 4: Asymmetrical fault at the middle of transmission line 6-9

Asymmetrical fault simulation is simulated to observe the response of the PtX due to this condition where the result obtained is compared to when symmetrical fault is injected to the system. The location of these fault simulations are the same, at the middle of transmission line 6-9 and both simulations have the same fault impedance. The type of asymmetrical fault considered in this simulation is line-to-ground (LG) fault. Figure 5.6 depicts the comparison of the response of the PtX due to the injection of LG fault and symmetrical fault

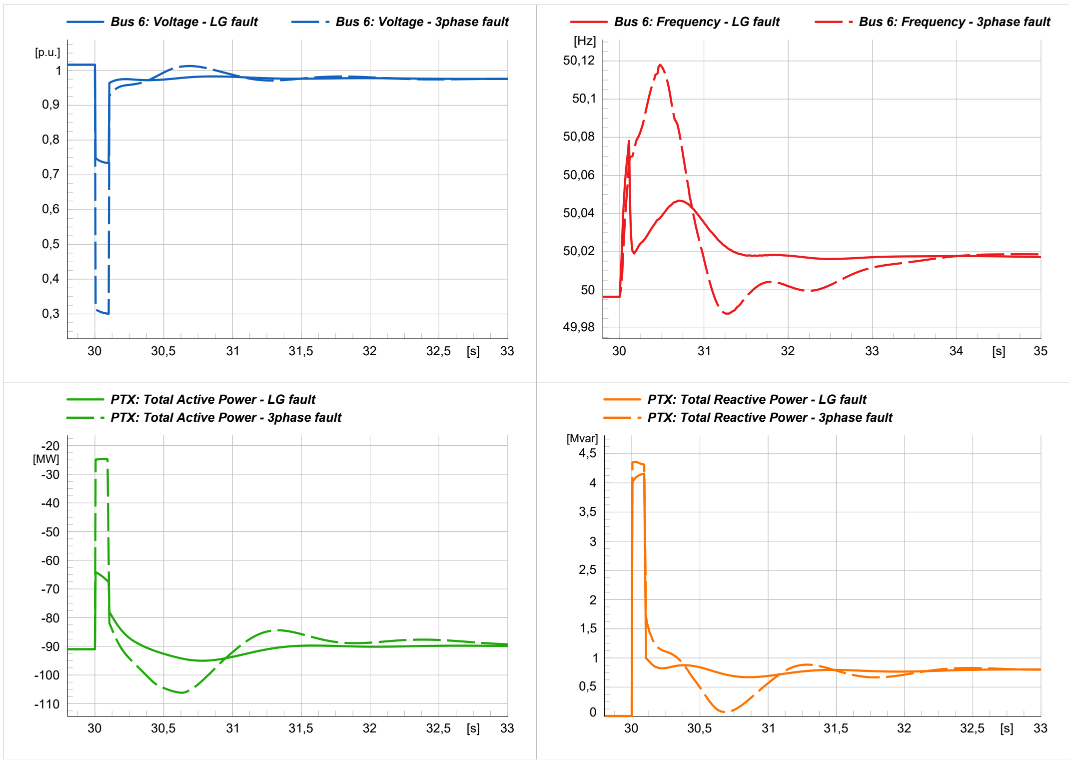

Figure 5.6: PtX response towards LG fault

From the result obtained shown in Figure 5.6, the voltage dip is larger for symmetrical fault. The frequency response towards LG fault do not deviate as large as for symmetrical fault. It also can be seen that the reduction of active power is less than for symmetrical fault. This is due to the phase affected is only a single phase for LG fault resulting in higher voltage measured at the terminal. This affects the output power regulated by the controller of PtX as described in Chapter 4.

The difference effect of LG fault in the system compared to symmetrical fault impact is shown in Figure 5.7. As the voltage do not drop drastically, the reactive power response from G1 does not get increased as high as for symmetrical fault. Whereas, the increase of measured frequency causes the active power to drop at during the fault condition. However, the oscillation of power for LG fault is not as large as symmetrical fault. The deviation on the speed and torque variables is also

smaller for LG fault due to the smaller impact to the voltage and frequency caused 1105
by the fault. In addition, the oscillation in the system is damped and it reaches steady state quicker for LG fault condition.

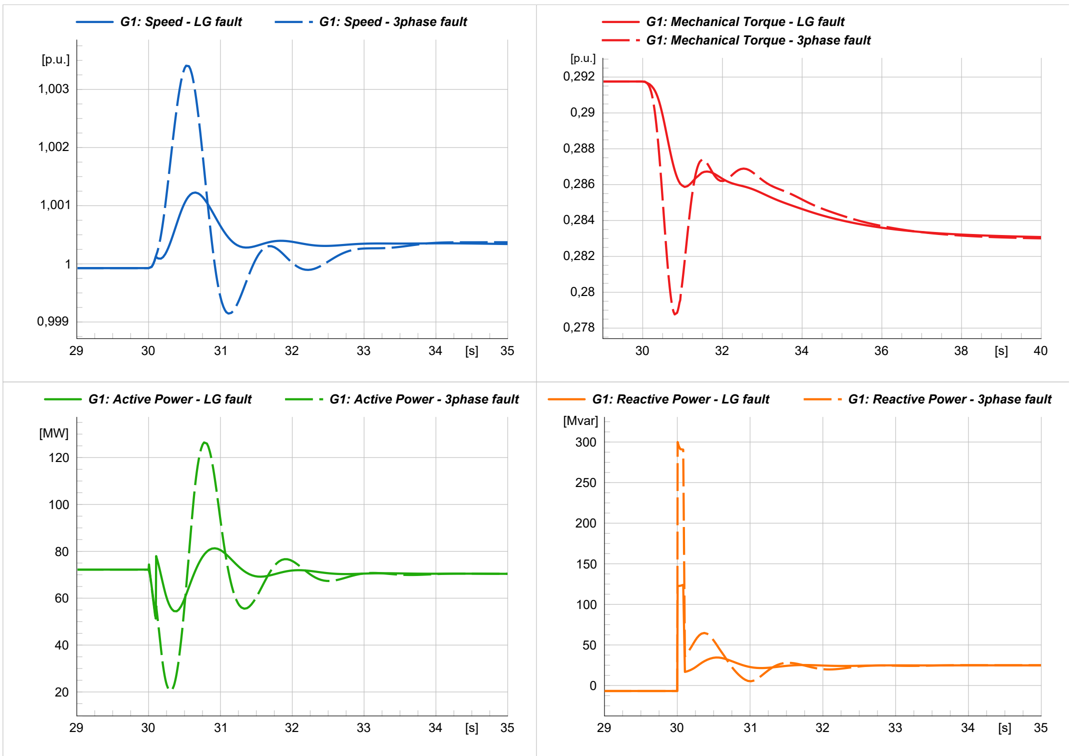

Figure 5.7: G1 response towards LG fault

5.6 Study test 5: Fault close to PtX

The simulation is run to observe the response of the PtX if the fault subject in the transmission line is closer to the PtX facility. The result obtained is compared with 1110
the result obtained for the fault injection at the middle of the transmission line. The fault type simulated for both cases is symmetrical fault. Figure 5.8 shows the comparison of the PtX response towards fault occurrence close to the PtX and at the middle of the line.

The result shows that the voltage detected by the PtX is lowered for fault oc- 1115
curing near the PtX facility compared to fault at the middle of the transmission line. This causes the PtX to decrease more its consumption of active power while it provides reactive power support to the grid. The frequency response shown for both simulation are relatively similar to each other as the fault type for both simulation are the same. As can be seen from the result of PtX response, the reactive 1120

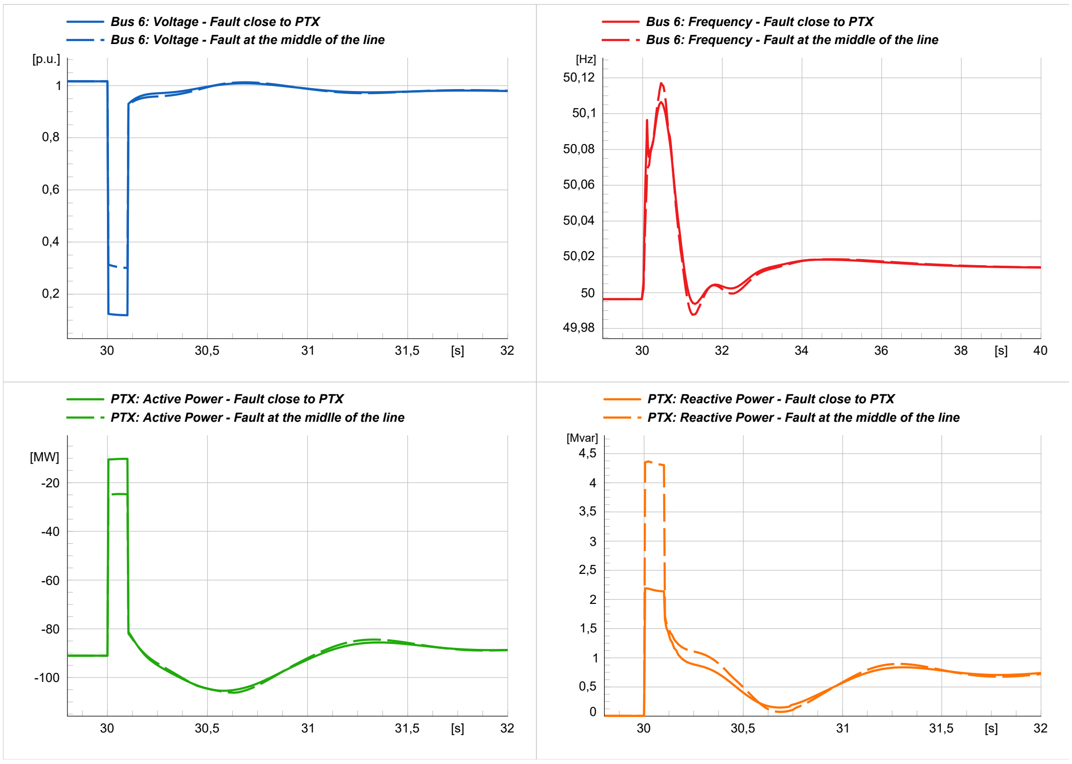

Figure 5.8: PtX response towards fault occurrence closer to PtX facility

power supported by the PtX is less for fault occurring near the PtX location. This is because G1 has an availability to supply higher reactive power to support the grid voltage.

The response of one of the SGs in the system, G1, is shown in Figure 5.9.

The response of G1 shows that the reactive power supplied is higher if the fault is located closer to the PtX facility. This is because the closer the fault to the PtX facility compared to the fault at the middle of transmission line 6-9, the fault is also closer to G1. This can be interpreted by G1 that the voltage drop at its terminal also is more lowered. Thus, G1 support the grid by supplying more reactive power.

Furthermore, the response on the speed of G1 is similar to for both simulations as the fault type occurring in the system are the same. This can also be observed on the torque and active power output of G1 as these variables are correlated to each other as described with eq. 3.2. However, although it is not significantly different, there still small difference on these measured variables. For instance, the small difference in active power output of G1 is caused by the response of active power output of the PtX during the fault injection. As the active power consumption is reduced more in the fault closer to the PtX facility, G1 regulates its output power to match the demand on the system,

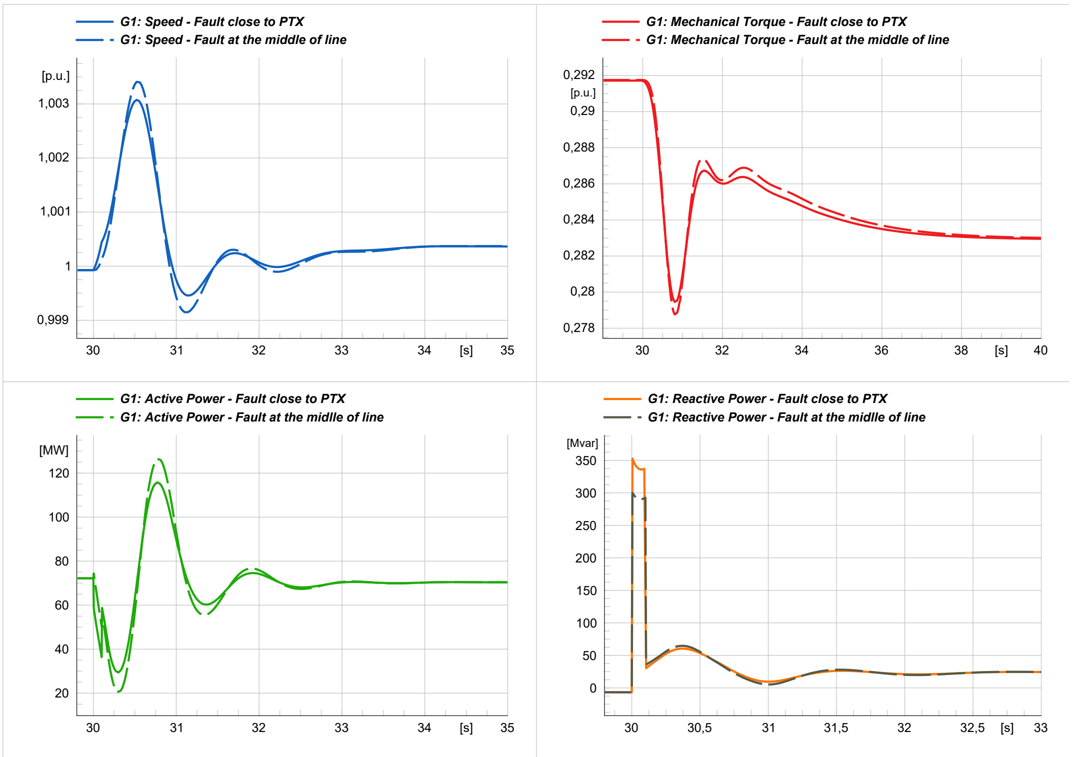

Figure 5.9: G1 response towards fault occurrence closer to PtX facility

5.7 Study test 6: Different location of PtX integration

The simulation is used to show the impact of PtX integration on the IEEE 9-bus system if it is located at different location/bus. The response of the PtX is different if the PtX is located at strong or weak grid system. From Table 3.6 and eq. 2.2, the SCR can be determined and thus, bus 4 is chosen to compare the impact of PtX integration at bus 6 if the fault occur in the system. The integration of PtX model at bus 4 holds higher SCR compared to PtX integration at bus 6. The fault injected is symmetrical fault located at the middle of transmission line 6-9, for both simulations. The PtX model is also set to consume same amount of power during pre-fault condition for both simulations.

Figure 5.10 shows the result of both fault simulations. During pre-fault condition, It can be seen that there is a small difference in the voltage magnitude measured in bus 6 for both simulations. This is due to different power flow through this bus of the two simulations. During fault, the voltage drop to very low value. This causes the PtX to supply higher reactive power compared to if the PtX located at bus 6.The measured frequency shown in the result explains the effect of the PtX integration at stronger SCR damped more compared to integration of PtX at weaker location. Thus, the active power response is less reduced for PtX located at bus 4 compared to bus 6. This is to maintain the frequency so it does not fluctuate largely.

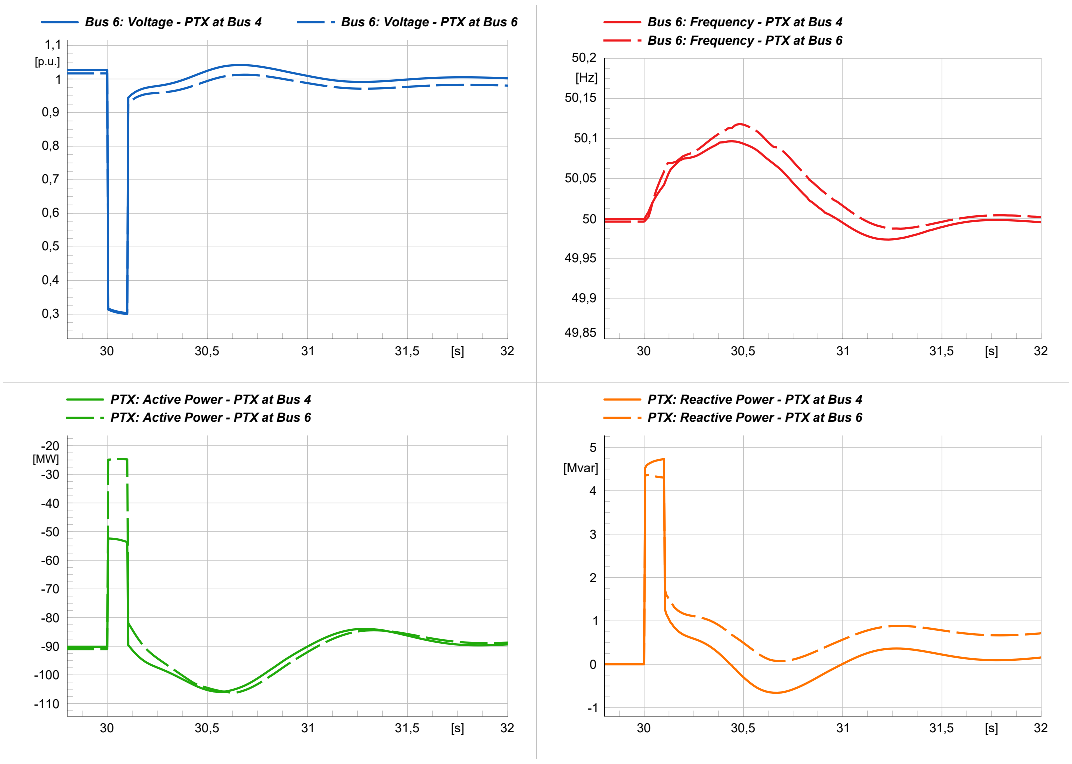

Figure 5.10: PtX response towards fault occurrence in transmission line if PtX is located differently

The impact of PtX integration at different location to the response of the system, represented by one of the SGs (G1), is shown in Figure 5.11. It can be seen that there is only slight difference of the response from G1 toward the fault occurring in the system. This is due to the same type of fault injection and at the exact same location. The difference for both simulations is mainly due to the contribution of PtX model to support the grid.

As the PtX reduces its active power consumption less when connected at bus 4, G1 also reduces its generation less. This result in the higher torque value until it reaches its steady state. However, the difference in the simulations is relatively small.

5.8 Study test 7: WTG implementation

This simulation is done to observe the response of PtX integration on weaker grid where the system consists of conventional power plants and renewable energy

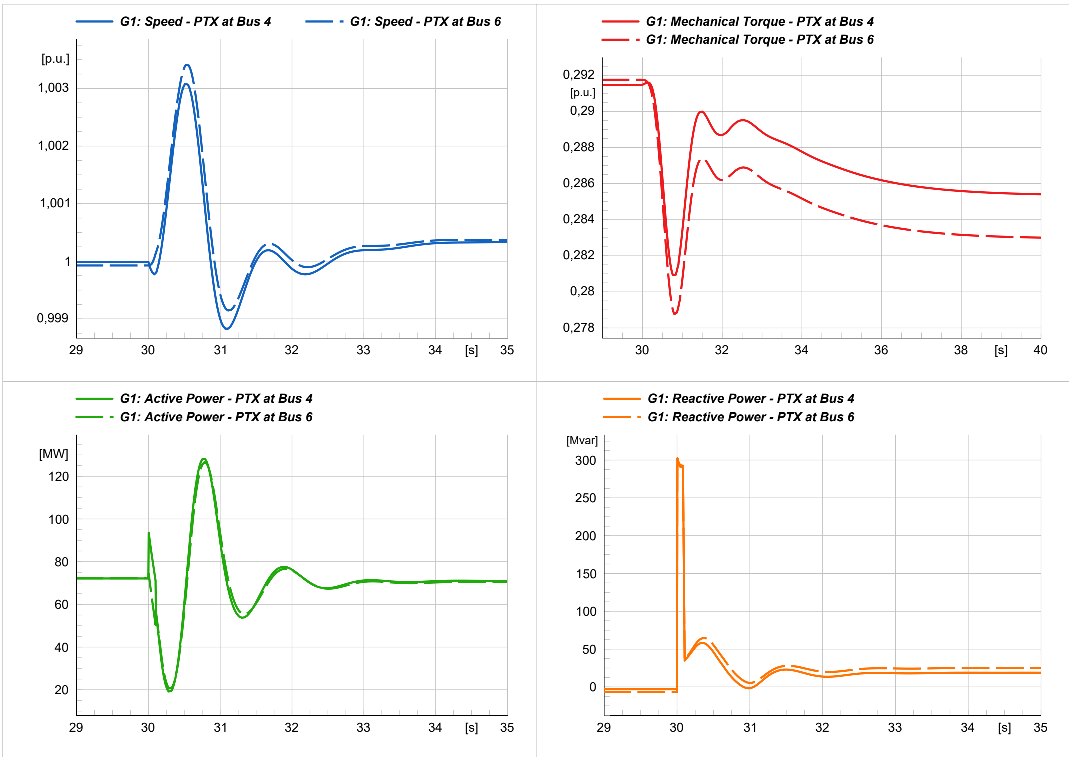

Figure 5.11: G1 response towards fault occurrence in transmission line if PtX is located differently

sources. This system is used to reflect more realistic grid system as it includes renewable energy sources. WTG substitutes one of the SGs in the IEEE 9-bus system where G3 is chosen to be replaced by the WTG. G3 is chosen to substituted by WTG as it is not the reference machine of the system and the location of G3 is close to PtX facility.

WTG model implementation is based on the WECC WT type 4A. PowerFactory has built-in model of this WTG with its dynamic model where the model from the database is considered as the WTG implemented in this study case. The WTG has an apparent power of 2 MVA. As the replaced G3 has a rated power of 128 MVA, the WTG model is aggregated so that the rated power of the WTG equals to G3 by assuming there are 64 WTG in parallel. The WECC WT type 4A has several controls including electrical control, named "REEC_A", for regulating its power, generator-converter model, named "REGC_A", for current control, and drive-train model, named "WTGT_A", for emulating the oscillation behaviour [55]. The parameter setting of WTG dynamic model is listed in Appendix C.

Due to the substitution of G3 with WTG, the SCR is different at each bus. The calculation of short-circuit power with WTG implemented in the IEEE 9-bus system is shown in Table D.1. Thus, it is determined that the PtX has weaker grid connection when the WTG is connected instead of G3. Transmission line 6-9 is short-circuited at the middle of the line to simulate this study case. The result is compared to when G3 is connected as in study case 1. The parameter for the simulation is the same as in study case 1, where the short-circuit type is symmetrical fault. Figure 5.12 shows the response of the PtX when symmetrical fault occurs in the system for both simulations, with WTG and with G3.

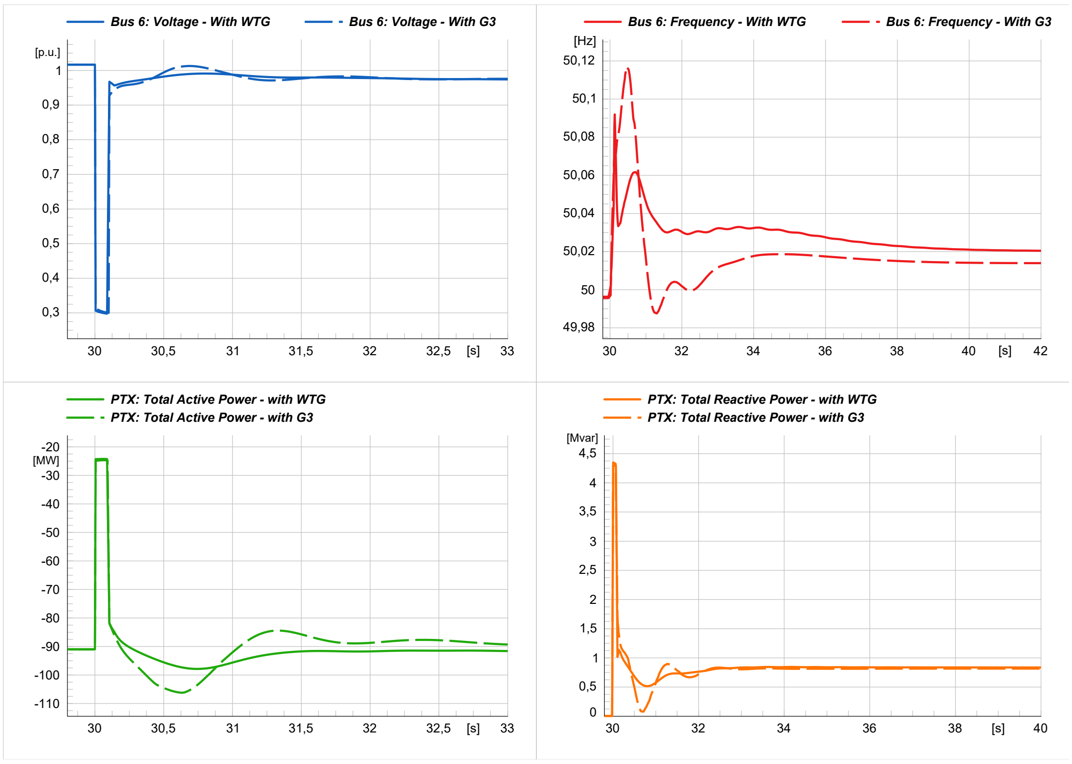

Figure 5.12: PtX response towards symmetrical fault for system consisting of WTG/G3

From the result of the PtX response, the active and reactive power of the PtX has more oscillations for system with G3 compared to the system with WTG. This might be caused due to the response of other SGs in the system towards this condition. However, the steady state point of the PtX after the fault clearance for active and reactive power are similar for simulations with WTG and G3. From the frequency measurement, it can be seen that for system using G3, although the frequency deviates larger during the fault period, the system can bring back the frequency to be close to its nominal frequency. Whereas, the frequency measured at the steady state after fault clearance is higher for system with WTG. To be noted, even though it can be seen that there is a difference on the frequency and voltage behaviour when G3 or WTG installed in the system, the difference is relatively small.

Figure **??** shows G1 response towards fault injection for simulation with WTG and G3. The result of G1 reflects the response of the PtX where the power supplied by G1 also oscillates with larger deviation for system deploying G3 compared to system with WTG. Due to the fault, the speed of G1 is also deviates larger but it could reach steady state closer to its pre-fault condition for system with G3 compared to system with WTG. This reflects in the torque of the G1. As the nominal speed of G1 at steady state after fault clearance for system with WTG is higher than system with WTG, the change in torque of G1 is also larger for system with WTG compared to system with G3.

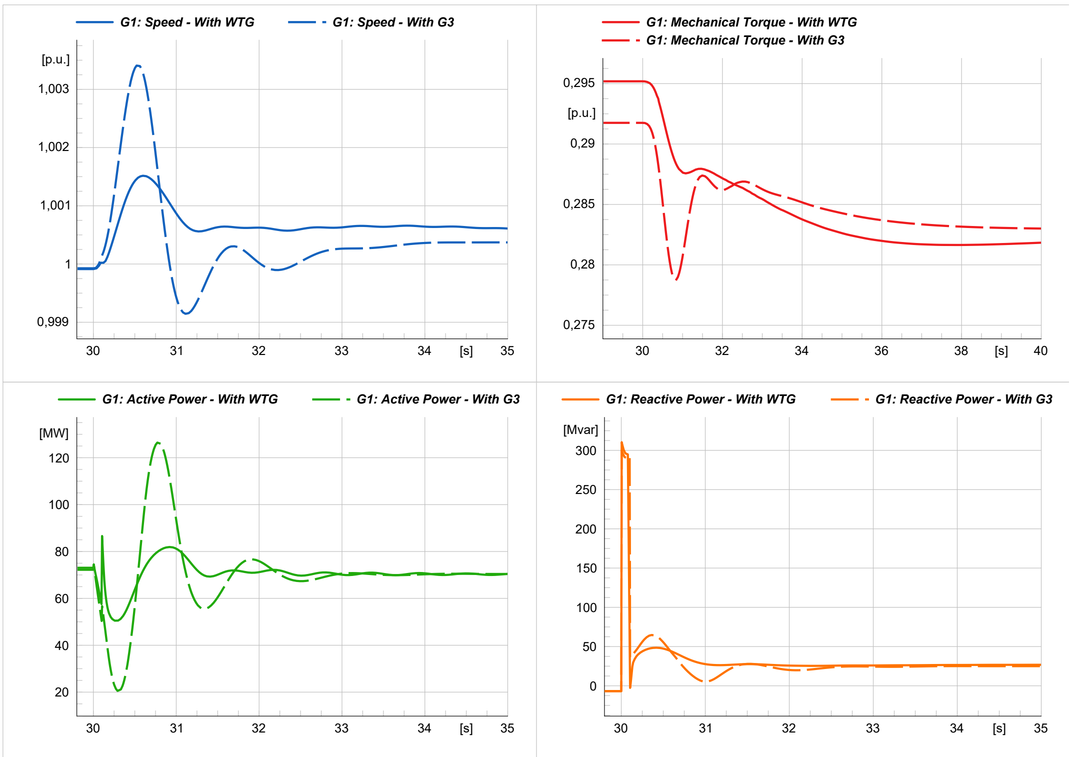

Figure 5.13: PtX response towards symmetrical fault for system consisting of WTG/G3

The different behaviour on the system with WTG and system with G3 can be explained by comparing the response of G3 and WTG towards the fault injection. Figure 5.14 plots the active and reactive power response of WTG and G3.

During the fault, the active power supplied by WTG is drop to almost zero while G3 can still maintain to generate active power although it is reduced. At the same time, G3 is capable to support the grid by supplying reactive power while the WTG could provide reactive power too but it is not as high as G3. After the fault is cleared, G3 and WTG operate as in pre-fault condition. However, due to the characteristic of G3 defined by its controller, the output power oscillates for a

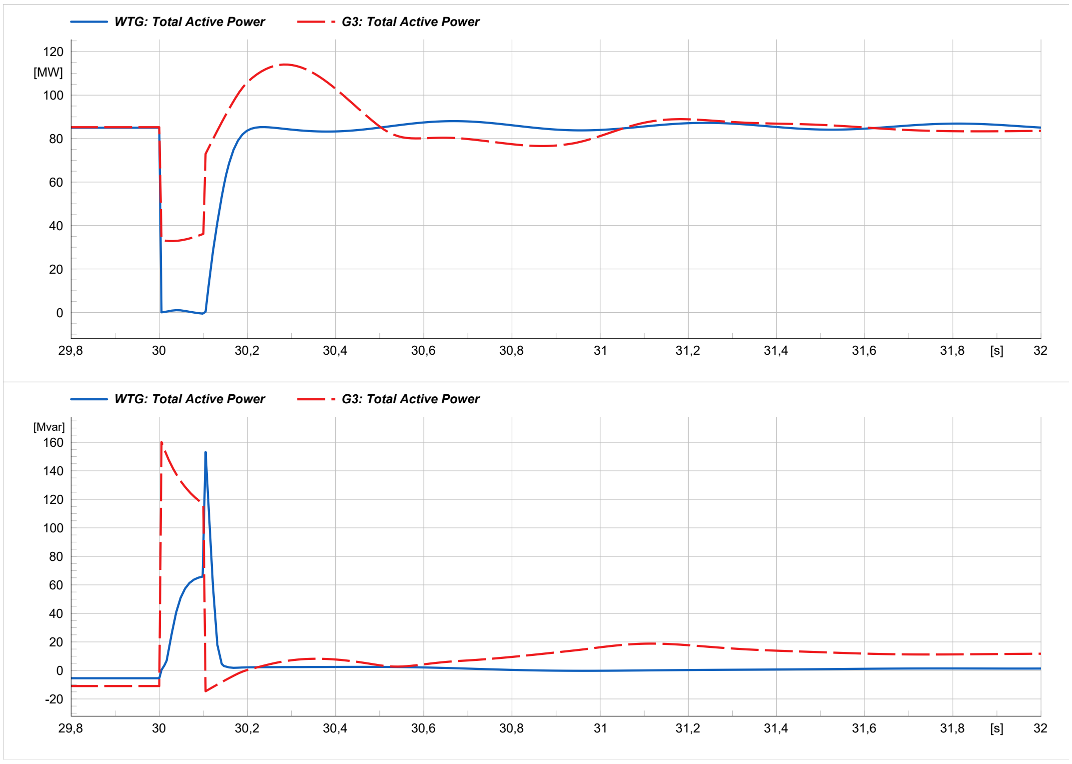

Figure 5.14: Comparison of WTG and G3 response response towards symmetrical fault

while. This results in better performance in the frequency as has been explained previously.

5.9 Conclusion

This chapter presents the result of PtX integration in the IEEE 9-bus system. Several schemes are undergone to observe the impact of the penetration of PtX in the system. Due to the setting of the controller for PtX, the model is able to provide services to the system to maintain the stability of the system by controlling the output power regulation of the PtX. The impact of the PtX has towards the system is it is able to maintain the voltage and frequency better compared to system without PtX implementation.

Chapter 6

Conclusion and Future Work

6.1 Result summary and conclusion

PtX technology is modelled in the simulation software to study the impact of the integration of this technology in the system. As the converter interfacing the electrolyzer to the grid should be able to operate based on the limitation of the electrolyzer, the PtX is modelled based on the electrolyzer converter. A grid following converter is considered to be the PtX model in this project.

As it is a grid following converter, the purpose of the controller of the model is to regulate its power output so that it could support the grid voltage and frequency. The control strategy implemented in the developed PtX model is through its innerloop current control where it regulates the PtX power output based on the implemented reversed droop control. The droop characteristic of the controller is determined from the droop setting from the system operator. It is also found out that PEM electrolyzer technology, as the benchmark in modelling the PtX, cannot supply active power to the grid. Thus, limiters are implemented in the current control model so that it would limit the PtX to not be able to supply power to the grid. Also, the reactive power is also limited based on the power capability of the technology used as the benchmark.

IEEE 9-bus system is used as the system for investigating the impact of the PtX integration where this is a small system consisted of three loads and three SGs. To represent the dynamic of the system properly, turbine-governor system and excitation system are modelled for each generation unit. The turbine-governor model helps in controlling the output power of the SGs while the excitation system controls the voltages at the terminal. PSS model is also included in dynamic model to damp the power swing due to disturbances occurring in the system. After modelling of the system, short-circuit power level is calculated to determine the location of PtX integration. It is found out that the the weakest part of the grid system is at bus 6. Thus, the PtX is placed at this bus to study the impact of the

PtX penetration.

Several schemes are simulated to observe the response of the PtX and also the impact to the system.

- The first simulation is comparing the response of PtX integration towards symmetrical fault to the response of a system without PtX implemented. The result shows that the the implementation of the developed PtX model could improve the performance of the system on the voltage and frequency of the system. This is because the PtX model could control its output power, both active and reactive.
- The second simulation is condition where the system loss one of its generation unit. The response of the PtX is compared to the response of the system without PtX. As the generation is disconnected from the grid system, the system experiences a drop of sources and thus the frequency drop. With PtX in the system, it could react fast enough to provide grid support service by reducing its active power. This result in better performance of the system frequency so that the frequency do not drop largely. Besides, it also provide reactive power supply to the grid so that it could maintain the voltage level.
- The third simulation is to show the response of the PtX model if it operates at its minimum.The result shows that the developed model limits its power output where it is constrained to not be able to supply active power to the grid.
- The remaining simulations show that the PtX could regulate the output power of the electrolyzer to operate accordingly to the condition in the grid system to help maintaining the stability.

Overall, the results show that there is an improvement in the performance of the system when PtX model is implemented. Thus, the PtX technology based on the implemented control could provide grid services to support the grid, such as the voltage and frequency, so that it could be stabilized faster towards disturbances in the system.

6.2 Future work

Based on the modelling of PtX on this project, an improvement for future work could be done, including:

- The system test used in this project is relatively a small system with only 3 SGs and 3 loads where the length to each bus location is equal. Other grid system can be used to investigate the impact of the PtX integration.

- Other type of fault or other locations for the fault injection could be considered to investigate the impact PtX towards this condition.

- Varying the type of the generation unit could also be considered for the next step of the project. As renewable energy plants are dominating the grid system in the recent years, the system could be adjusted so that the it is dominated by these sources where the impact of PtX integration will be different compared to a system with dominant conventional power plant.

- Other control strategy of beside using droop control could be implemented to see the response of the PtX system. For example, the control mode implemented could be for voltage control or power factor control.

- The modelling of PtX model could also consider a grid forming converter where it has different control structure to grid following converter.

Bibliography

[1] European Commission. *Behavioural Climate Change Mitigation Options and Their Appropriate Inclusion in Quantitative Longer Term Policy Scenarios*. Apr. 2012. URL: https://ec.europa.eu/clima/system/files/2016-11/main_report_en.pdf.

[2] The Climate Partnership for the Energy and Utilities Sector. *Powering Denmark's Green Transition*. May 2020. URL: https://www.danskenergi.dk/sites/danskenergi.dk/files/media/dokumenter/2020-07/Powering_Denmarks_Green_Transition_Climatepartnership.pdf.

[3] Thomas Weiss Anders N. Andersen Peter Sorknæs Henning Mæng. *Overview of the Danish Power system and RES integration*. July 2013. URL: https://www.store-project.eu/documents/target-country-results/en_GB/energy-needs-in-denmark-executive-summary.

[4] Danish Energy Agency. *Energy Statistics 2020*. 2021. URL: https://ens.dk/sites/ens.dk/files/Statistik/energy_statistics_2020.pdf.

[5] Hans-Kristian Ringkjøb, Peter M. Haugan, and Ida Marie Solbrekke. "A review of modelling tools for energy and electricity systems with large shares of variable renewables". In: *Renewable and Sustainable Energy Reviews* 96 (2018), pp. 440–459. ISSN: 1364-0321. DOI: https://doi.org/10.1016/j.rser.2018.08.002. URL: https://www.sciencedirect.com/science/article/pii/S1364032118305690.

[6] Giulio Buffo et al. "Chapter 15 - Power-to-X and power-to-power routes". In: *Solar Hydrogen Production*. Ed. by Francesco Calise et al. Academic Press, 2019, pp. 529–557. ISBN: 978-0-12-814853-2. DOI: https://doi.org/10.1016/B978-0-12-814853-2.00015-1. URL: https://www.sciencedirect.com/science/article/pii/B9780128148532000151.

[7] Energinet. *Winds of Change in A Hydrogen Perspective, PtX strategic Action Plan*. 2019. URL: https://en.energinet.dk/About-our-reports/Reports/PtX_strategic_action_plan.

[8] Energinet. *System Perspective 2035 Long-term perspectives for efficient use of renewable energy in the Danish energy system*. 2018. URL: https://en.energinet.dk/systemperspective2035.

[9] Energinet. *Appendix to System Perspective 2035, Modelling of Energy Plants*. 2018. URL: https://en.energinet.dk/systemperspective2035.

[10] Christina Wulf, Petra Zapp, and Andrea Schreiber. "Review of Power-to-X Demonstration Projects in Europe". In: *Frontiers in Energy Research* 8 (2020). ISSN: 2296-598X. DOI: 10.3389/fenrg.2020.00191. URL: https://www.frontiersin.org/article/10.3389/fenrg.2020.00191.

[11] Energy Danish Ministry of Climate and Utilities. *The Government's strategy for POWER-TO-X*. 2021. URL: https://ens.dk/sites/ens.dk/files/ptx/strategy_ptx.pdf.

[12] Energy Danish Ministry of Climate and Utilities. *Denmark's Energy Islands*. URL: https://ens.dk/en/our-responsibilities/wind-power/energy-islands/denmarks-energy-islands.

[13] Rahman Daiyan, Iain MacGill, and Rose Amal. "Opportunities and Challenges for Renewable Power-to-X". In: *ACS Energy Letters* 5.12 (2020), pp. 3843–3847. DOI: 10.1021/acsenergylett.0c02249. eprint: https://doi.org/10.1021/acsenergylett.0c02249. URL: https://doi.org/10.1021/acsenergylett.0c02249.

[14] Lingguo Kong, Jiamin Yu, and Guowei Cai. "Modeling, control and simulation of a photovoltaic /hydrogen/ supercapacitor hybrid power generation system for grid-connected applications". In: *International Journal of Hydrogen Energy* 44.46 (2019). Special Issue on International Conference on Novel Functional Materials 2018, pp. 25129–25144. ISSN: 0360-3199. DOI: https://doi.org/10.1016/j.ijhydene.2019.05.097. URL: https://www.sciencedirect.com/science/article/pii/S0360319919319536.

[15] H. Tebibel et al. "Design, modelling and optimal power and hydrogen management strategy of an off grid PV system for hydrogen production using methanol electrolysis". In: *International Journal of Hydrogen Energy* 42.22 (2017), pp. 14950–14967. ISSN: 0360-3199. DOI: https://doi.org/10.1016/j.ijhydene.2017.05.010. URL: https://www.sciencedirect.com/science/article/pii/S0360319917318025.

[16] Mengxing Chen et al. "Overview of Power Electronic Converter Topologies Enabling Large-Scale Hydrogen Production via Water Electrolysis". In: *Applied Sciences* 12.4 (2022). ISSN: 2076-3417. DOI: 10.3390/app12041906. URL: https://www.mdpi.com/2076-3417/12/4/1906.

[17] Helma Maria Trondheim et al. “Frequency and Voltage Analysis of the Hybrid Power System in Suðuroy, Faroe Islands”. English. In: *Proceedings of the Virtual 5th International Hybrid Power Systems Workshop*. Virtual 5th International Hybrid Power Systems Workshop ; Conference date: 18-05-2021 Through 19-05-2021. Energynautics GmbH, May 2021. URL: https://hybridpowersystems.org/.

[18] JWG C4/C6.35/CIRED. *Modelling of Inverter-based Generation for Power System Dynamic Studies*. 2018. URL: https://e-cigre.org/publication/727-modelling-of-inverter-based-generation-for-power-system-dynamic-studies.

[19] Florin Iov, Mahmood Khatibi, and Jan Dimon Bendtsen. “On the Participation of Power-To-Heat Assets in Frequency Regulation Markets—A Danish Case Study”. In: *Energies* 13.18 (2020). ISSN: 1996-1073. DOI: 10.3390/en13184608. URL: https://www.mdpi.com/1996-1073/13/18/4608.

[20] Shi You et al. “Facilitating Water electrolysers for electricity-grid services in Europe through establishing standardized testing protocols”. In: *Clean Energy* 4.4 (Nov. 2020), pp. 379–388. ISSN: 2515-4230. DOI: 10.1093/ce/zkaa015. eprint: https://academic.oup.com/ce/article-pdf/4/4/379/35924660/zkaa015.pdf. URL: https://doi.org/10.1093/ce/zkaa015.

[21] R. D’hulst et al. “Voltage and frequency control for future power systems: the ELECTRA IRP proposal”. In: *2015 International Symposium on Smart Electric Distribution Systems and Technologies (EDST)*. 2015, pp. 245–250. DOI: 10.1109/SEDST.2015.7315215.

[22] Manish Mohanpurkar et al. “Electrolyzers Enhancing Flexibility in Electric Grids”. In: *Energies* 10.11 (2017). ISSN: 1996-1073. DOI: 10.3390/en10111836. URL: https://www.mdpi.com/1996-1073/10/11/1836.

[23] Bang L. H. Nguyen et al. “Power Converter Topologies for Electrolyzer Applications to Enable Electric Grid Services”. In: *IECON 2021 – 47th Annual Conference of the IEEE Industrial Electronics Society*. 2021, pp. 1–6. DOI: 10.1109/IECON48115.2021.9589044.

[24] Nicola Chiesa et al. “Dynamic control of an electrolyser for voltage quality enhancement”. In: *Proc. Int. Conf. on Power System Transients (IPST-11)* (Jan. 2011).

[25] Mehdi Ghazavi Dozein, Ahvand Jalali, and Pierluigi Mancarella. “Fast Frequency Response From Utility-Scale Hydrogen Electrolyzers”. In: *IEEE Transactions on Sustainable Energy* 12.3 (2021), pp. 1707–1717. DOI: 10.1109/TSTE.2021.3063245.

[26] Xuetao Xing et al. "Modeling and operation of the power-to-gas system for renewables integration: a review". In: *CSEE Journal of Power and Energy Systems* 4.2 (2018), pp. 168–178. DOI: 10.17775/CSEEJPES.2018.00260.

[27] Energinet. *Technical Regulation 3.3.1 for Electrical Energy Storage Facilities*. 2019. URL: ttps://en.energinet.dk/Electricity/Rules-and-Regulations/Regulations-for-grid-connection.

[28] Guangsheng Pan et al. "Optimal Planning for Electricity-Hydrogen Integrated Energy System Considering Power to Hydrogen and Heat and Seasonal Storage". In: *IEEE Transactions on Sustainable Energy* 11.4 (2020), pp. 2662–2676. DOI: 10.1109/TSTE.2020.2970078.

[29] M.N. Manage et al. "A techno-economic appraisal of hydrogen generation and the case for solid oxide electrolyser cells". In: *International Journal of Hydrogen Energy* 36.10 (2011), pp. 5782–5796. ISSN: 0360-3199. DOI: https://doi.org/10.1016/j.ijhydene.2011.01.075. URL: https://www.sciencedirect.com/science/article/pii/S0360319911001182.

[30] Xuetao Xing et al. "Modeling and operation of the power-to-gas system for renewables integration: a review". In: *CSEE Journal of Power and Energy Systems* 4.2 (2018), pp. 168–178. DOI: 10.17775/CSEEJPES.2018.00260.

[31] Takaya Ogawa, Mizutomo Takeuchi, and Yuya Kajikawa. "Analysis of Trends and Emerging Technologies in Water Electrolysis Research Based on a Computational Method: A Comparison with Fuel Cell Research". In: *Sustainability* 10.2 (2018). ISSN: 2071-1050. DOI: 10.3390/su10020478. URL: https://www.mdpi.com/2071-1050/10/2/478.

[32] O. Schmidt et al. "Future cost and performance of water electrolysis: An expert elicitation study". In: *International Journal of Hydrogen Energy* 42.52 (2017), pp. 30470–30492. ISSN: 0360-3199. DOI: https://doi.org/10.1016/j.ijhydene.2017.10.045. URL: https://www.sciencedirect.com/science/article/pii/S0360319917339435.

[33] Siemens Energy. *Workshop PtG/PtL, Large Scale PEM Electrolysis and Sector Coupling*. 2020. URL: https://www.heattofuel.eu/wp-content/uploads/2021/03/6_Ilona-Dickschas.pdf.

[34] Arunkumar Pandiyan et al. "Review of solid oxide electrolysis cells: a clean energy strategy for hydrogen generation". In: *Nanomaterials and Energy* 8.1 (2019), pp. 2–22. DOI: 10.1680/jnaen.18.00009. eprint: https://doi.org/10.1680/jnaen.18.00009. URL: https://doi.org/10.1680/jnaen.18.00009.

[35] European Commission. *Electrolyzer Service Catalogue*. Nov. 2017. URL: https://cordis.europa.eu/project/id/735485/results.

[36] Bart W. Tuinema et al. “Modelling of large-sized electrolysers for real-time simulation and study of the possibility of frequency support by electrolysers”. In: *IET Generation, Transmission & Distribution* 14.10 (2020), pp. 1985–1992. DOI: https://doi.org/10.1049/iet-gtd.2019.1364. eprint: https://ietresearch.onlinelibrary.wiley.com/doi/pdf/10.1049/iet-gtd.2019.1364. URL: https://ietresearch.onlinelibrary.wiley.com/doi/abs/10.1049/iet-gtd.2019.1364.

[37] Xiangjun Quan et al. “Control of grid-forming application for fuel cell/electrolyser system”. In: *IET Renewable Power Generation* 14.17 (2020), pp. 3368–3374. DOI: https://doi.org/10.1049/iet-rpg.2020.0508. eprint: https://ietresearch.onlinelibrary.wiley.com/doi/pdf/10.1049/iet-rpg.2020.0508. URL: https://ietresearch.onlinelibrary.wiley.com/doi/abs/10.1049/iet-rpg.2020.0508.

[38] JTF IEEE/CIGRE. *Definition and classification of power system stability*. 2003. URL: https://e-cigre.org/publication/231-definition-and-classification-of-power-system-stability.

[39] Jahangir Hossain and Hemanshu Roy Pota. *Robust control for grid voltage stability: high penetration of renewable energy : interfacing conventional and renewable power generation resources*. eng. Power systems. Springer, 2014. ISBN: 9789812871152.

[40] Lasantha Meegahapola et al. “Power System Stability with Power-Electronic Converter Interfaced Renewable Power Generation: Present Issues and Future Trends”. In: *Energies* 13.13 (2020). ISSN: 1996-1073. DOI: 10.3390/en13133441. URL: https://www.mdpi.com/1996-1073/13/13/3441.

[41] DIgSILENT GmbH. *DIgSILENT PowerFactory Version 2021: User Manual*. Mar. 2021. URL: https://www.digsilent.de.

[42] Arrillaga Jos Watson Neville. Institution of Engineering and Technology (The IET), 2019. ISBN: 978-1-78561-499-6. URL: https://app.knovel.com/hotlink/toc/id:kpPSETSE02/power-systems-electromagnetic/power-systems-electromagnetic.

[43] North American Electric Reliability Cooperation. *Short-Circuit Modeling and System Strength*. Feb. 2018. URL: https://www.nerc.com.

[44] Mehdi Ghazavi Dozein et al. “System Strength and Weak Grids: Fundamentals, Challenges, and Mitigation Strategies”. In: *2018 Australasian Universities Power Engineering Conference (AUPEC)*. 2018, pp. 1–7. DOI: 10.1109/AUPEC.2018.8757997.

[45] P. M. Anderson. *Power system control and stability*. eng. IEEE press power engineering series. Hoboken: John Wiley Sons Inc, 2003. ISBN: 0471238627.

[46] DIgSILENT GmbH. *Nine-bus System*. 2021. URL: `https://www.digsilent.de`.

[47] John J. Grainger. *Power system analysis.* eng. McGraw-Hill series in electrical and computer engineering. New York,N.Y: McGraw-Hill, 1994. ISBN: 0070612935.

[48] "IEEE Recommended Practice for Conducting Load-Flow Studies and Analysis of Industrial and Commercial Power Systems". In: *IEEE Std 3002.2-2018* (2018), pp. 1–73. DOI: `10.1109/IEEESTD.2018.8529292`.

[49] Task Force on Turbine-Governor Modeling. *Dynamic Models for Turbine-Governors in Power System Studies*. Jan. 2013. URL: `https://site.ieee.org/fw-pes/files/2013/01/PES_TR1.pdf`.

[50] Prabha. Kundur. *Power systems stability and control.* eng. EPRI power system engineering series. New York, N.Y: Mcgraw-Hill, 1994. ISBN: 9780070359581.

[51] "IEEE Recommended Practice for Excitation System Models for Power System Stability Studies". In: *IEEE Std 421.5-2005 (Revision of IEEE Std 421.5-1992)* (2006), pp. 1–93. DOI: `10.1109/IEEESTD.2006.99499`.

[52] Anton Janssen et al. "Operating experience with and future challenges for coordinating power plant and power system protection". In: *Cigre Science Engineering* 7 (Feb. 2017), p. 63.

[53] Dan Wu et al. "Control and analysis of droop and reverse droop controllers for distributed generations". In: *2014 IEEE 11th International Multi-Conference on Systems, Signals Devices (SSD14)*. 2014, pp. 1–5. DOI: `10.1109/SSD.2014.6808842`.

[54] Vasile-Simion Sularea. *Design and control of high efficiency wind turbine based hydrogen production system*. eng. 2016.

[55] Electric Power Research Institute (EPRI). *Type 4 - Generic Wind Turbine Generator Model (Phase II)*. URL: `https://www.esig.energy/wiki-main-page/type-4-generic-wind-turbine-generator-model-phase-ii/`.

Appendix A

Email from Siemens Energy

Emne: WG: Large scale P2X - studenterprojekt med Energinet

Dear Peter,
Attached please find the answers on the questions, that had been send.

1. Type of the electrolyzer ....PEM
2. Rated power and voltage .... 7,8 kA at 800 V DC per rectifier
3. PQ capability ... typically cos(phi) > 0.95 with compensation
4. FRT capability ... in development
5. Control functions of the electrolyzer....main functions are temperature, level, current, and H2/O2 pressure control
6. Response time of the electrolyzer.....10%/s in normal operation regime, limited for very low load

Hope that suits the purpose. If not, please get back to me.
Greetings
Eric

Appendix B

Parameter of Power-to-X Controller

Reverse Droop Control Paramater

Table B.1: Reverse droop control parameter

Parameter	Description	Value
mr	Reactive power droop coefficient [-]	0.05
nr	Reactive power droop coefficient [-]	0.05
w_c	Low pass filter cut-off frequency [rad/s]	75400

Current Control Parameter

Table B.2: Current control parameter

Parameter	Description	Value
Kd	Gain active current controller [-]	0.62
Td	Integrator time constant active current control [s]	0.01
Kq	Gain reactive current controller [-]	0.62
Tq	Integrator time constant active current control [s]	0.01
$\mathrm{idref}_m in$	Minimum reference current d-axis	-105
$\mathrm{idref}_m ax$	Maximum reference current d-axis	0
$\mathrm{iqref}_l im$	Maximum/minimum reference current q-axis	32.786

Appendix C

WECC WT Type 4A Control Parameter

Renewable Energy Electrical Controller (REEC$_A$)*Parameter*

Table C.1: REEC control parameter

Parameter	Description	Value
PfFlag	Power factor control flag, 1 = pf ctrl, 0 = Q control	0
VFlag	Voltage control flag, 1 = Q ctrl, 0 = voltage control	0
Tp	Filter time constant for power measurement [s]	0.05
KqP	Proportional gain [p.u.]	1
Kqi	Integral gain [p.u.]	0.7
QFlag	Q control flag: 1 = voltage/Q, 0 = const. pf or Q ctrl.	1
Kvp	Proportional gain [p.u.]	1
Kvi	Integral gain [p.u.]	0.7
Trv	Filter time constant for voltage measurement [s]	0.01
db1	Voltage deadband for overrvoltage iq injection [p.u.]	-0.05
db2	Voltage deadband for undervoltage iq injection [p.u.]	0.05
Kqv	Gain for Reactive current injection during fault [p.u.]	2
Thld	Reactive current injection delay after voltage dip [s]	0
Vdip	Undervoltage condition trigger voltage [p.u.]	0.9
Vup	Overvoltage condition trigger voltage [p.u.]	1.1
Tiq	Time constant on lag delay [s]	0.01
Tpord	Time constant [s]	0.01
PqFlag	Priority flag on current limit: 1 = P, 0 = Q priority	0
Imax	Maximum converter current limit [p.u.]	1.3
Thld2	Ipcmd$_{m}axdelayafterfault[s]$	0
PFlag	Power control flag: 0 = P,1 = Speed ref.	1
Vref0	Reference voltage, enter 0 for terminal voltage [p.u.]	0
Vref1	User-defined ref./bias on inner-loop voltage ctrl. [p.u.]	0
Iq$_{f}rz$	Value at which injection is held after voltage dip [p.u.]	0
Qmin	Reactive power limit minimum [p.u.]	-0.436
Vmin	Voltage control minimum [p.u.]	0.9
Iql1	Minimum limit of reactive current injection [p.u.]	-1.1
dPmin	Ramp rate on power reference [p.u./s]	-2
Pmin	Minimum power reference [p.u.]	0
Qmax	Reactive power limit maximum [p.u.]	0.436
Vmax	Voltage control maximum [p.u.]	1.1
Iqh1	Maximum limit of reactive current injection [p.u.]	1.1
dPmax	Ramp rate on power reference [p.u./s]	2
Pmax	Maximum power reference [p.u.]	1

Appendix D

Short-circuit Power for System with WTG

Table D.1: Short-circuit power of IEEE 9-bus system with WTG

Bus	Short-circuit power [MVA]
Bus 1	1582.2
Bus 2	1419.7
Bus 3	547.5
Bus 4	1129.3
Bus 5	855.8
Bus 6	754.7
Bus 7	1093.5
Bus 8	798.2
Bus 9	687.6
Bus WT	422.1